1.1 Astronomy in the radio band.

It is well known tat the Earth atmosphere is opaque to most of electromagnetic (e.m.) radiation and that the only two non-blocked atmospheric windows are the optical and radio bands (Fig. 1[1]).

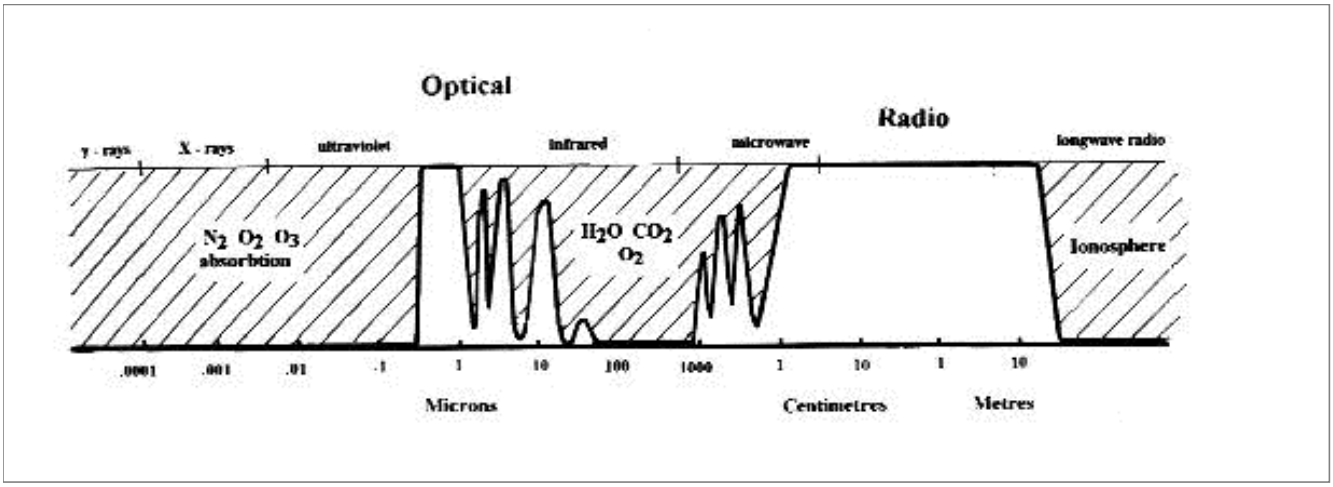


Figure 1: The electromagnetic spectrum

The visible band goes from 0.4 to 0.7 micron. It is therefore narrow, blocked at the ultraviolet (UV) end by ozone, oxygen and nitrogen absorption, at the infrared (IR) end manly by water vapor and carbon dioxide. Only a small part of IR photons can be observed from below the atmosphere, and in any case from high and dry mountain sites. In most of the IR band balloons or even satellite are required. Concerning the UV band and the shortest X-ray and γ wavelengths, photons are completely blocked by the atmosphere, requiring the use of satellites for extra-terrestrial observations.

The lowest energy photons fall instead in the *radio window*, which is usually divided into several sub-bands: HF (below 30 MHz – above 10 m), VHF (30-300 MHz, 1-10 m), UHF (300-1000 MHz, 0.3-1 m), microwave (1000-30000 MHz, 0.01-0.3 m), millimeter and sub-millimeter wave (the microwave regime, at the border with the FIR part of the e.m. spectrum). At mm wavelengths the frequency of radiation is very close to the vibration and rotation frequency of oxygen molecules in water vapor. Therefore, a variable fraction of radiation can be absorbed as a function of the atmospheric humidity. The presence of clouds can therefore generate problems for observations in the

1 This figure, as well as many of the others that you will find in the following, are extracted from different WEB pages. I acknowledge all the authors.

shortest part of the radio band. At intermediate wavelengths (cm-m) the atmospheric humidity is not a problem. At longer radio wavelengths (≥ m) the ionosphere reflects and, in part, absorbs the e.m. incoming radiation. The ionization of these layers of the atmosphere is due to the activity of the Sun. A critical frequency exists above which the ionized medium reflects completely the incoming radiation. The value of such a frequency strongly depends on the activity of the Sun, the time and the place of observations. In optimal conditions, observations can be done up to about 35 m.

Today radioastronomy is one of the main branch of modern astronomy, even if its history is much shorter if compared to other wavelengths, in particular the visible band (for obvious reasons: men have always had an optical detector – their eyes – while radio telescopes are quite recent – the last century). Actually, for many thousands of years mankind was restricted to observations of visible light, since astronomers were limited either by the terrestrial atmosphere (X-ray, UV, most of IR band) or by the lack of detectors for different kind of radiations (radio band). We now know very well that, in order to be able to study and understand the astrophysical mechanisms responsible for the emission and evolution of all the different sources of radiation in the Universe, a multi-wavelength "eye" is absolutely necessary.

For example, our Galaxy (the Milky Way) is an assembly of stars of different ages, which are embedded in an *inter-stellar medium* (ISM) made by ionized and neutral gas. Due to their temperature range, at optical wavelengths we can observe the surface of stars and the nearby ionized gas.



Figure 2: Optical image of the Milky Way

The clearly visible dark patches present in Fig. 2 are due to absorbing clouds of gas and dust, which are evident in the infrared (Fig. 3) and molecular hydrogen (Fig. 4) maps as emission regions. Actually, part of the ISM particles are able to absorb the optical light and to re-emit the absorbed photons at IR wavelengths. Therefore most of the IR emission shown in Fig. 3 is thermal, from interstellar dust warmed by absorbed starlight.

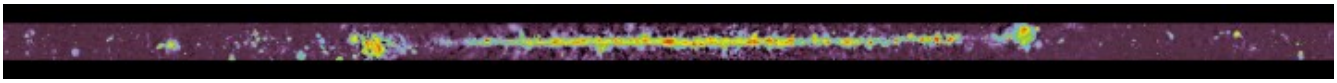


Figure 3: IR image of the Milky Way

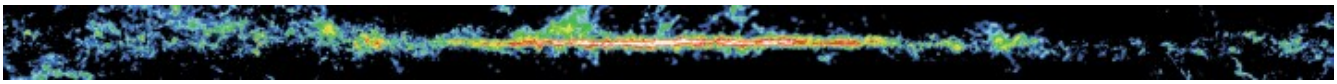


Figure 4: Molecular clouds in the Milky Way

Column density of molecular hydrogen inferred from the intensity of the J =1-0 spectral line of carbon monoxide, a standard tracer of the cold, dense parts of the interstellar medium, is shown in Fig. 4. Such gas is concentrated in the spiral arms in discrete "molecular clouds." Most molecular clouds are sites of star formation. The image in Fig. 4 has been observed at 115 GHz (i.e. mm wavelengths).

Radio astronomy addresses a broad range of phenomena, including the radiation from the 21 cm line of neutral hydrogen (Fig. 5) and the thermal radiation from a wide variety of molecular lines, coming from dense, extremely cold gas concentrations that are found within the ISM. Some non-thermal radio emission has also been detected from the Milky Way (Fig. 6). It is synchrotron radiation coming from charged particles, usually electrons, with very high energies, moving at relativistic velocities in the magnetic field of the ISM. Here the term "*thermal*" implies that there is some approximation to an equilibrium, or quasi-equilibrium, condition in the emitting medium, with the components of the gas showing an approximated Maxwell-Boltzmann velocity distribution.

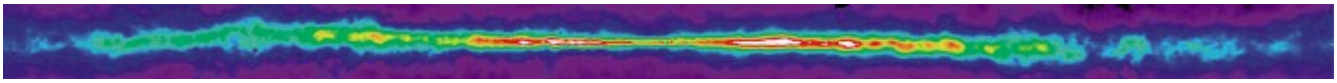


Figure 5: 21 cm observations of the Milky Way (atomic hydrogen emission)

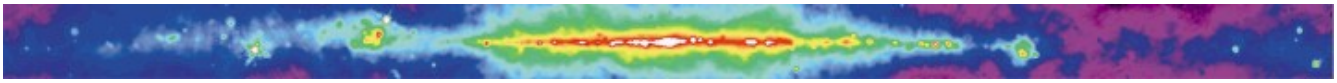


Figure 6: Radio continuum emission from the Milky Way (408 MHz)

In 1931, Jansky's discovery of radio emission from the Milky Way paved the way for the new science of radioastronomy. In the 50's and 60's, the first radio maps of our Galaxy showed the presence of radio emission from the supernova remnants like the Crab Nebula, new supernova-related objects like Cassiopeia A, but also revealed extra-galactic objects, such as nearby peculiar galaxies like M87 and very distant radio galaxies like Cygnus A. The possibility of mapping the 3D spatial distribution of neutral hydrogen through 21 cm observations allowed to discover the spiral structure of our Galaxy. Millimetric observations revealed one of the most important discovery of modern Cosmology: the microwave background, fossil black-body radiation of the primordial Universe, when its temperature was about 3° K (about 380 thousands years after the Big Bang, estimated to happen 13.7 billion years

ago). These photons, emitted during the first main phase transition of the Universe's life, when radiation and matter decoupled, allow us to trace the seed of all the structures that we observe now, from stars and planets, to clusters and super-clusters of galaxies (Fig. 7).

Not only radioastronomy gives a complementary view of the different astrophysical objects compared to the visible band, but its different observational technique allow us to reach significantly higher sensitivity limits (i.e. weaker and/or more distant sources) due to a larger collecting area of radio telescopes compared to optical instruments. Larger telescopes are absolutely essential in radioastronomy in order to have angular resolutions comparable to optical telescopes. Actually, there are no differences in the behavior of optical and radio waves; in principle, we could therefore use telescopes similar to optical instruments to observe radio sources. However, we will see that the angular resolution of a telescope of size D is proportional to λ/D, λ being the observing wavelength. Since radio wavelengths are about 1 million time higher than optical wavelengths, giant radio telescopes are necessary to reach angular resolutions similar to those of optical instruments (characterized by D of the order of 1-10 m). Hence, the necessity of developing the interferometric technique in radio astronomy, which, as we will see, combines different antennae in order to reach a total instrument size of the order of kilometers. Another important properties of radio telescopes is that they measure the energy received from a distant source (as do all the other astronomical observations), but before the radio energy is measured (*detection*), the e.m. wave properties are retained and operated on. An e.m. wave has both amplitude and phase. While the simplest detection process takes only the square of the amplitude and lose the phase information, with radio telescopes the relative phase properties of the incoming e.m. waves can be inferred.

In this lecture, I will give you an introduction about radioastronomy, starting from some basic concepts about radioastronomical observations and data analysis. The main mechanisms responsible for emission at radio wavelengths will also be presented. I will finally give you an overview of the main galactic and extra-galactic radio sources.

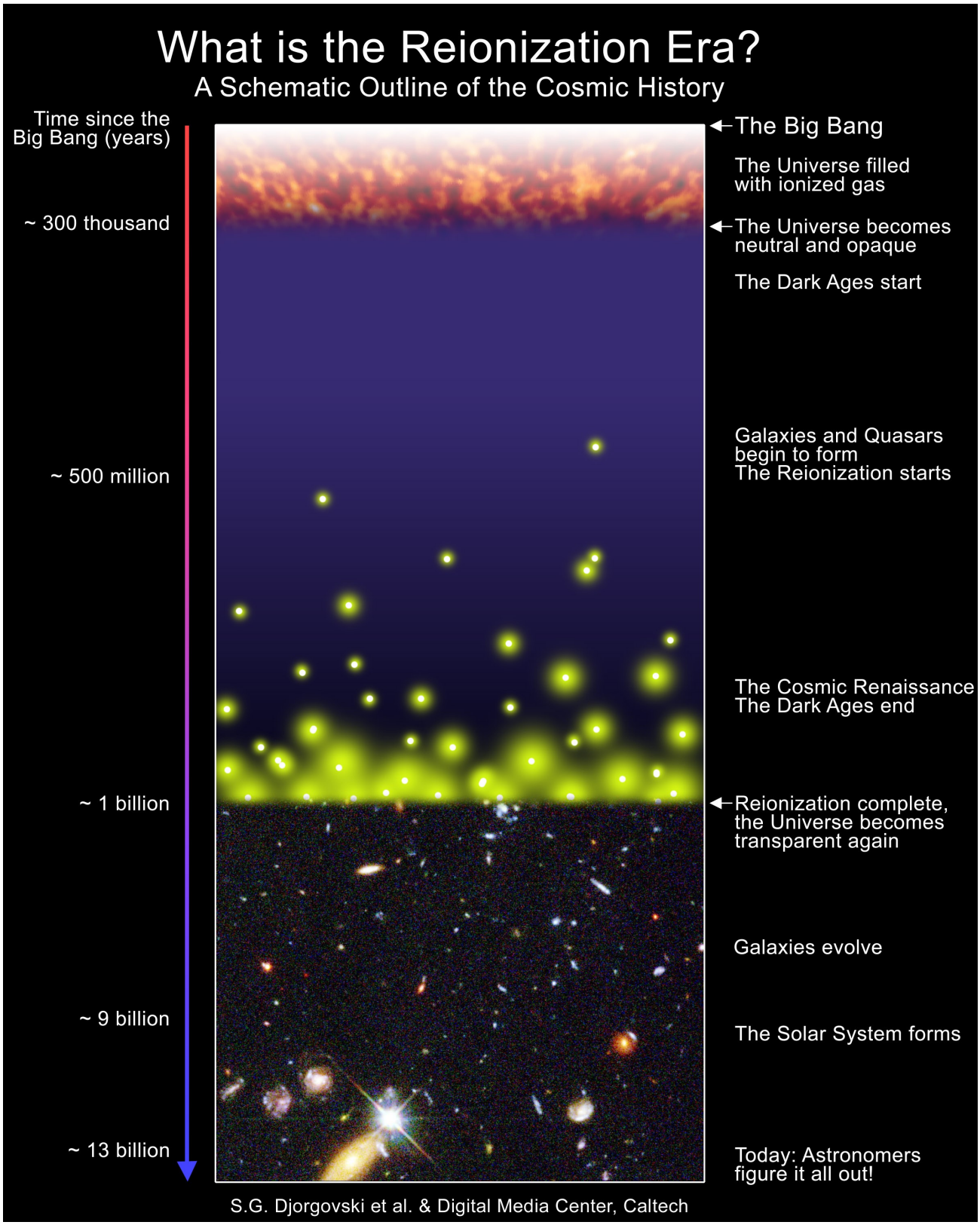


Figure 7: A schematic outline of the cosmic history

1.2 Electromagnetic waves

Radio observations, as all astronomical observations, consist of measuring the energy received from a distant sources. But, while simple detection processes (as optical observations) takes the square of the amplitude of the incoming electromagnetic wave, at radio wavelengths the electromagnetic wave properties (amplitude and phase) are retained and operated on before the radio energy is measured (detection phase). In radio astronomy, the incoming wave is transformed to electrical signals by the telescope, signals that can be, for instance, amplified and cross- correlated with other radio signals.

We will shortly summarize here the main properties of e.m. radiation. In free space, the propagation of e.m. waves is governed by the wave equation, that, for the electric field $\vec{E}$ is:

$$\nabla^2 \vec{E} = \frac{1}{c^2} \frac{\partial^2 \vec{E}}{\partial t^2} \tag{1.1}$$

The magnetic field $\vec{B}$ obeys a similar equation and lies perpendicular to the magnetic field. The cross product $\vec{E} \times \vec{B}$ determines the direction of propagation $\vec{z}$.

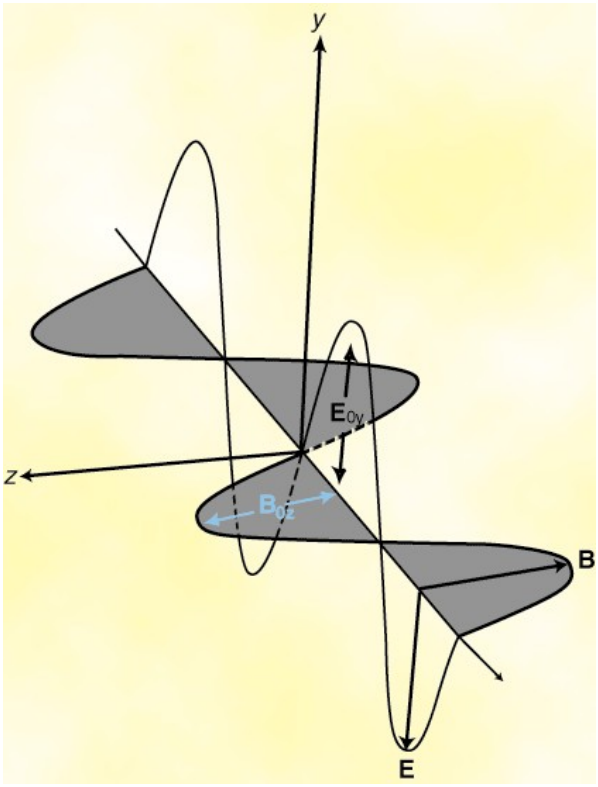


Figure 8: Electromagnetic wave

Near the source of radiation, Eq. (1.1) requires spherical waves, but astronomical sources are at

great distance and the curvature of the wavefront is negligible. This means that plane waves are a sufficiently good approximation. This is always true in the case of sources at astronomical distances, for which the *far field condition* ($R_{ff} \gg \frac{D^2}{\lambda}$, R_{ff} being the distance of the source emitting radiation at a wavelength λ from a telescope of size D) is always satisfied.

A monochromatic transverse wave, with $\vec{E}$ in the direction of a unit vector $\hat{a}$, propagates along the direction $\vec{z}$ with wavelength λ, frequency ν (=c/λ , c being the speed of light) and phase ϕ (the phase being zero at the origin of time and space).

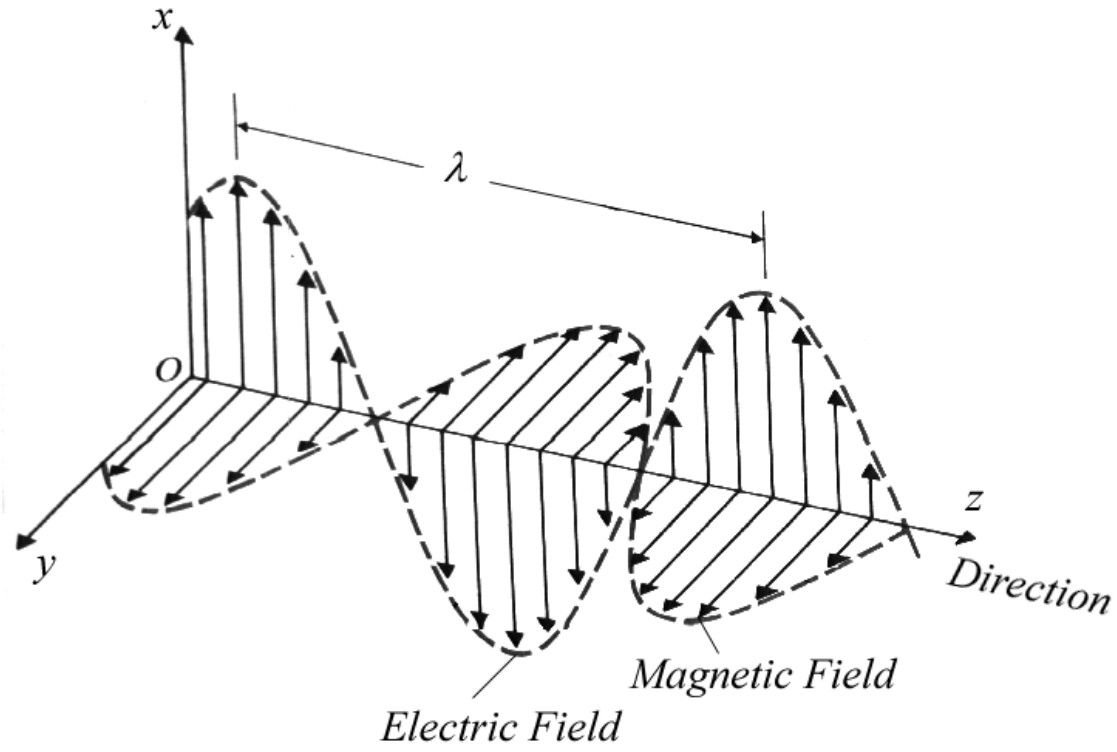


Figure 9: Wavelength of an electromagnetic wave

Such a wave will take the simple form:

$$\vec{E}(x,y)=\hat{a}\,E_0\cos(2\pi(\nu t - z/\lambda)+\Phi)$$

or, in complex notation, with E_0 now containing the phase:

$$\vec{E}(x,y)=\hat{a}\,E_0\exp(i2\pi(\nu t - z/\lambda))$$

The vector $\hat{a}$, perpendicular to the direction of propagation and parallel to $\vec{E}$, defines the polarization directions. If $\hat{a}$ has a constant orientation as the wave propagates, the wave is *linearly polarized*. However, the electric field vector can be arbitrarily divided into two perpendicular

components. If they are in phase we are in the previously defined case (*linear polarization*, Fig.9). The electric vector is the sum of the two components and its direction is constant. This direction depends on the relative amplitude of the two components. If the two components have the same amplitude and they are exactly 90° out of phase, one component is zero when the other is at maximum or minimum amplitude. This special case is called *circular polarization* (Fig. 11, right hand or left hand depending on the way the electric vector rotates). In all the other cases, that is is the two components are not in phase and either do not have the same amplitude and/or are not 90° out of phase, we have *elliptical polarization* (Fig.11).

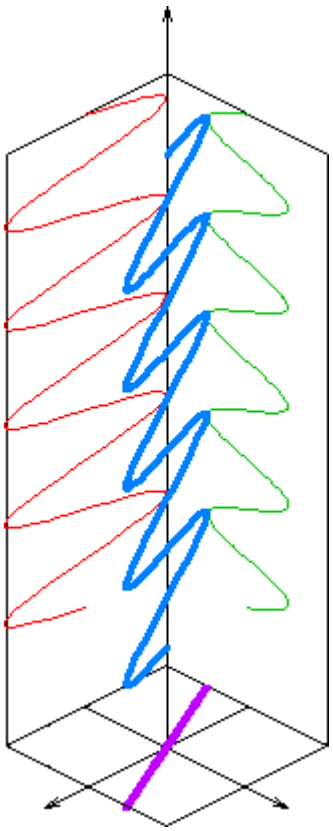


Figure 10: Linear polarization

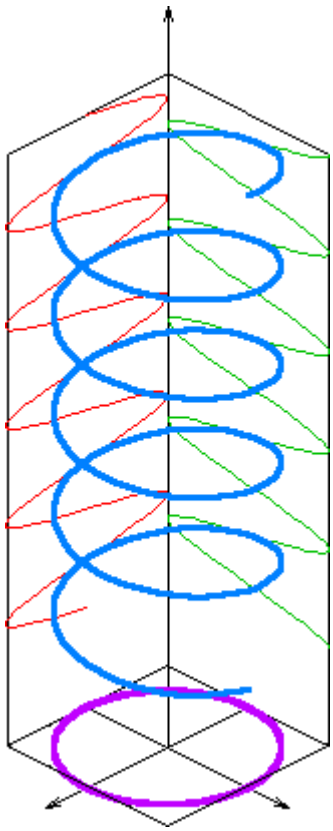


Figure 11: Circular polarization

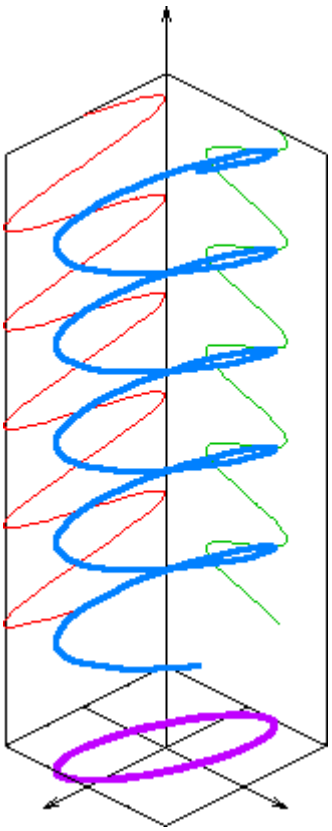


Figure 12: Elliptical polarization

1.3 Some basic definitions: brightness, flux density, brightness temperature.

Electromagnetic radiation is a wave phenomenon. The propagation of e.m. waves is governed by the wave equation, which requires spherical waves near the source. However, astronomical sources are at great distances, and the curvature of the wavefront is negligible. The infinitesimal power dW intercepted by an infinitesimal surface dA is:

$$dW = B_\nu (dA \cos\theta) d\,\Omega\, d\,\nu \qquad \text{(watts)} \qquad (1.2)$$

where:

dW	=	infinitesimal power (watts)
B_ν	=	surface brightness or specific intensity (watts m^{-2} Hz^{-1} sr^{-2})
$d\Omega$	=	infinitesimal solid angle (= senθ dθ dϕ, sr^2)
dA	=	infinitesimal area of surface (m^2)
θ	=	angle between the normal to dA and the direction to $d\Omega$
$dA\ cos\theta$	=	projection of dA on the plane perpendicular to the incident radiation (m^2)
$d\nu$	=	infinitesimal bandwidth (Hz)

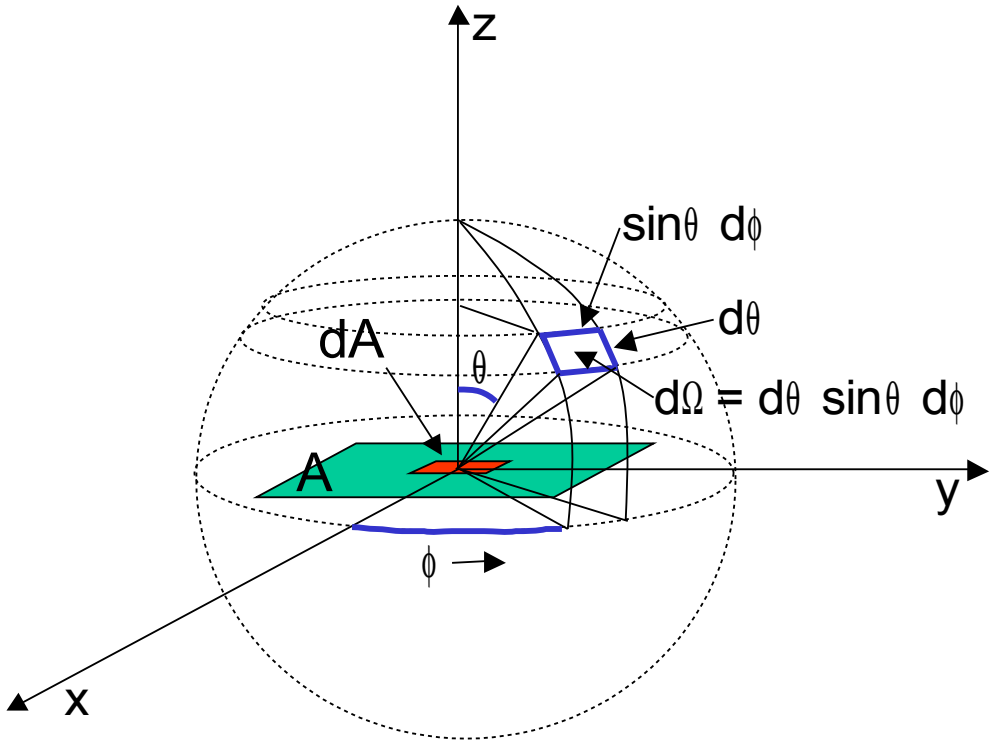


Figure 13: A sketch to illustrate the definition of brightness

Equation (1.2) gives the definition of the *(surface) brightness* B_ν. It represents the power received per unit area, per unit solid angle, per unit bandwidth. The variation of the brightness with frequency ($B(\nu)$) is called *brightness spectrum*. In general the brightness variates also from one position to another in the sky (i.e. $B=B(\nu,\theta,\phi)$).

By integrating equation (1.2) over the total solid angle subtended by the source (Ω_S) we obtain the total power W received in a frequency range $\Delta\nu$[2]:

$$W = \int_{\Delta\nu} \iint_{\Omega_s} B(\nu)\, dA \cos\theta\, d\Omega\, d\nu \qquad \text{(watts)} \tag{1.3}$$

Usually, the *specific power* or *power density* (i.e. power per unit bandwidth) is given:

$$dw = B(\nu)\, d\Omega\, dA \cos\theta \qquad \text{(watts/Hz)} \tag{1.4}$$

Its variation with frequency is called *spectrum* of the radio source. The shape of observed spectra depends on different physical properties of the source of radio waves (e.g. the mechanisms responsible for the acceleration of electrons, the age of the source, its morphology, etc.).

The quantity measured by radio telescopes is actually the *spectral flux density* (or simply *flux*) of a source[3]:

$$S(\nu) = W(\nu) / 4\pi d^2$$

where d is the distance of the radio source.

It is obtained by integrating the surface brightness over the total solid angle subtended by the source (Ω_S):

$$S_\nu = \int_{\Omega_s} B_\nu(\theta,\phi)\, d\Omega \qquad \text{(watts m}^{-2}\text{ Hz}^{-1}\text{)} \tag{1.5}$$

2 This quantity, integrated from 0 to ∞, corresponds to the quantity called "absolute luminosity" at optical wavelengths.
3 The so called "apparent luminosity" at optical wavelengths.

Since the flux density of radio sources is usually very small, a special radio astronomical flux density unit, the *Jansky* (*Jy*) has been introduced:

$$1\ \text{Jy} = 10^{-26}\ \text{watts m}^{-2}\ \text{Hz}^{-1} = 10^{-23}\ \text{erg s}^{-1}\ \text{cm}^{-2}\ \text{Hz}^{-1} \qquad (1.6)$$

Very few extra-galactic radio sources are as bright as 1 Jy. It has therefore to be stressed the huge sensitivity of radio telescopes: a flux of 1Jy is comparable to the flux received on Earth from a 100 watt lamp on the Moon.

An important property of the surface brightness is that it is independent of the distance to the source [4]. It only depend on the size and emissivity of the radiating source. Consider a volume dv of matter, at a distance r from us, that emits e.m. radiation with an emission coefficient j (W/Kg/Hz). The power emitted in the frequency range dν is given by:

$$dW = j\,\rho\,dv\,d\,\nu$$

where ρ is the density of matter (Kg/m^3). The brightness is thus given by:

$$dB = \frac{dW}{4\pi r^2}\frac{1}{d\,\Omega}\frac{1}{d\,\nu} = \frac{j\,\rho\,dv\,d\,\nu}{4\pi r^2 d\,\Omega d\,\nu} = \frac{j\,\rho\,dv}{4\pi r^2 d\,\Omega} \qquad (1.7)$$

Since: $dv = r^2\,dr\,d\,\Omega$, Eq. (1.7) becomes:

$$dB = \frac{j\,\rho\,dr}{4\pi}$$

For a finite width of the emitting material, the brightness is given by:

$$B = \frac{1}{4\pi}\int_{r1}^{r2} j\,\rho\,dr$$

4 As long as the effects of diffraction and extinction can be neglected.

that does not depend at all from the distance of the source from us. This can also be understood in a more intuitive way: if the radio source is twice more distant, the power received on Earth is 4 times lower (due to the inverse square dependence from distance); but also dΩ is 4 times lower. Therefore, for the same values of dA and dν, the brightness derived from Eq. (1.5) does not depend on the distance of the source from us.

Radio astronomers often express the brightness of a source as a *temperature*. This is due to the fact that the spectral distribution of the radiation of a black body in thermodynamic equilibrium (given by the Planck law):

$$B_\nu(T)=\frac{2\mathrm{h}\,\nu^3}{c^2}\frac{1}{\mathrm{e}^{h\nu/kT}-1} \tag{1.8}$$

at radio frequencies falls in the Rayleigh-Jeans regime ($h\nu \ll kT$, $\mathrm{e}^{h\nu/kT}\simeq 1+\frac{h\nu}{kT}+\ldots$):

$$B_{RJ}(\nu,T)=\frac{2\nu^2}{c^2}kT \tag{1.9}$$

This implies that, in the radio band, the brightness and the thermodynamic temperature of the emitting black body are strictly proportional. This feature is so useful that it has become the custom in radio astronomy to measure the brightness of an extended source by its *brightness temperature* T_b, derived from equation (1.9):

$$T_b=\frac{c^2}{2\mathrm{k}}\frac{1}{\nu^2}B_\nu \tag{1.10}$$

T_b is therefore the temperature at which a black body would have to be in order to radiate the observed brightness B_ν . If B_ν is emitted by a black body and $h\nu \ll kT$, Eq. (1.10) indeed gives the thermodynamic temperature of the source, a value that is independent of ν. But if other processes are responsible for the emission of the radiation (as it is generally the case of radio sources), T_b does not correspond to a real physical temperature. It is, however, still a useful quantity for practical work.

1.4 Fraunhofer diffraction and its applications.

Diffraction is a phenomena arising from the wave nature of light. A diffraction pattern appears because light will interfere with itself. Diffraction occurs when waves pass through small openings, around obstacles, or past sharp edges. *Fraunhofer diffraction* occurs when both incident and diffracted waves are plane. To create such a situation, one must make the distance from the light source to the diffracting obstacle to the observation point large enough to neglect the curvature of incident and diffracted light (i.e. far field condition seen above). In other words, when the light reaches the diffracting aperture, the spherical wavefront should be large enough that it is virtually a planar wave front (basically a flat, vertical line) over it. The rays must then be parallel, or close to parallel, as they reach the diffracting object. The point at which the diffraction pattern is observed becomes the *Fraunhofer plane*.

Why are we interested to Fraunhofer diffraction now? Because, as we will see in the following, it allows us to introduce one of the most important concept in radio observations, that is the concept of *antenna pattern* (or *power pattern* or *beam*). When we have to deal with image reconstruction in astronomy, the first thing to be taken into account is the *diffraction pattern* of the observational instrument. The diffraction pattern describes how the energy of an incoming plane wave distributes on the focal plane of the instrument, and it assumes different names in the different bands of the e.m. spectrum. In optical, the diffraction pattern is called *Point Spread Function* (*PSF*), at radio wavelengths *antenna pattern* (or *power pattern* or *beam*), in the X-ray band *efficiency*. These differences in the adopted nomenclature depend on the kind of instruments originally used in the different bands (e.g. a circular mirror in optical, an antenna at radio wavelengths).

The PSF can be quite difficult to be determined *a priori*, even if some analytical expressions, which give good approximations, are known. However, in the case of optical telescopes, the diffraction pattern is usually estimated by observing stars, whose image produced by the instrument corresponds to the diffraction pattern due to a point source, i.e. the instrument PSF. The diffraction pattern can on the contrary be easily determined based on the instrument properties when we are in the approximation of Fraunhofer diffraction.

Consider a single aperture (e.g. an antenna) of width *a,* reached by a monochromatic e.m. wave. At the time *t*, the electric field on a generic point of the aperture will be given by:

$$F(x)\cos(\nu t-\phi(t)) \tag{1.11}$$

where ν is the monochromatic frequency of the radiation, $F(x)$ and $\phi(t)$ its amplitude and phase respectively. If the wave is plane (as we will assume being in the far field domain, see Fig. 14), $F(x)=const.$ and $\phi(t)=const.$ This electric field transmitted by the aperture is called *grading* (or *aperture distribution*).

If we adopt the complex formalism, we can re-write the grading as:

$$g(x)=F(x)\mathrm{e}^{-i\phi(t)}\mathrm{e}^{i\nu t} \tag{1.12}$$

Remember that we are interested only to the real part of Eq. (1.12).

Consider now what happens at time $t=t_0$, which we can assume to be 0, on a plane parallel to the aperture and located at a distance significantly higher (~∞, *Fraunhofer plane)* than the aperture dimension (far field condition, see Fig. 14).

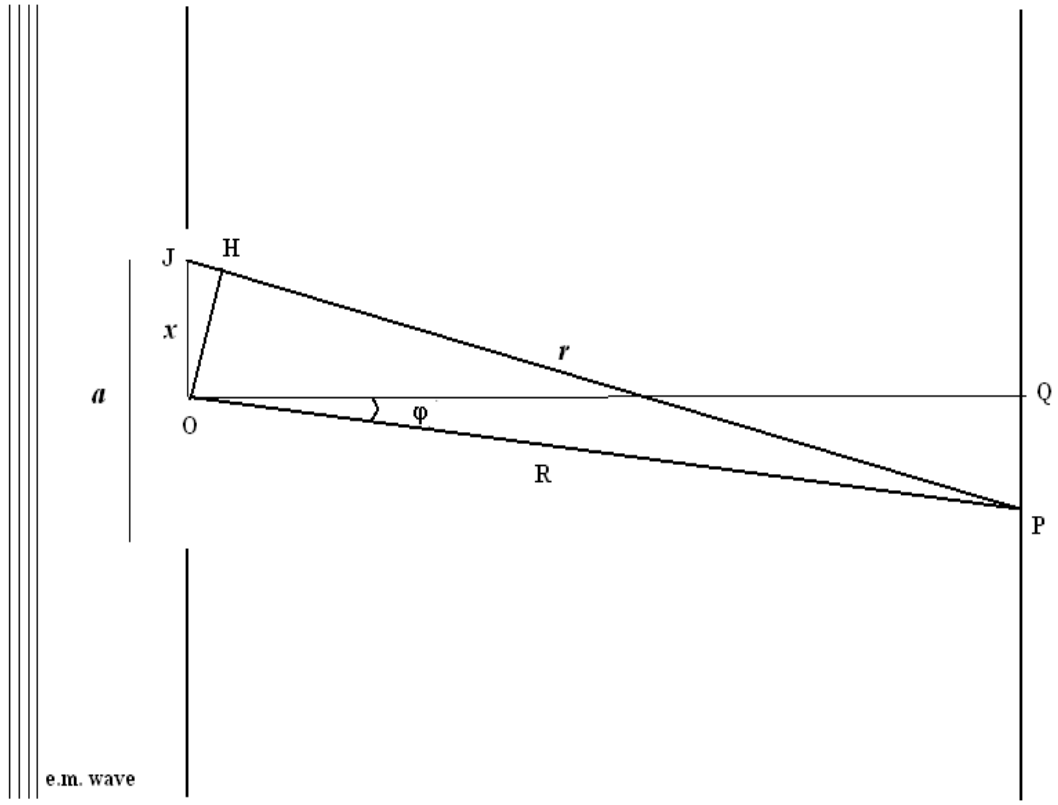


Figure 14: Single aperture (of width a) scheme

$\overline{OP} = R \simeq \overline{HP}$ (assuming that we are in the far field domain $r \gg \frac{a^2}{\lambda}$, with $r \to \infty$)

$\overline{JP} = r$

$\overline{JO} = x$

$\overline{JH} = x \sin\varphi$

According to *Huyghens' principle* (see Fig. 15), every wavefront point on the aperture is a source of secondary wavelets. The electric field on each point of the Fraunhofer plane is thus given by the sum of the values that the resulting electric fields (i.e. those produced in every single point of the aperture by to the incoming waves) assume in that point of the Fraunhofer plane.

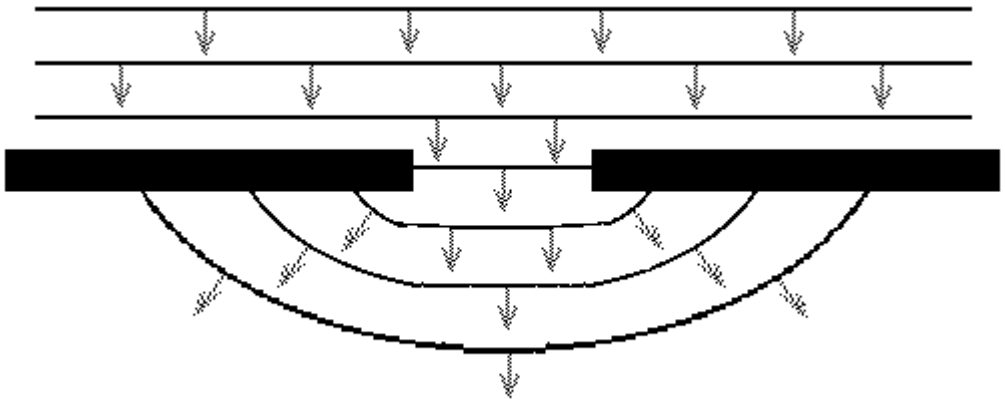


Figure 15: Huyghens' principle

The electric field originated in a point P of the screen (see Fig. 14) by the spherical wave coming from a generic point dx of the aperture (point located at a distance x from the center of the aperture) is:

$$dE = g(x)\mathrm{e}^{-2\pi i r/\lambda}\,dx \tag{1.13}$$

where r is the distance from dx (indicated by the letter J in Fig. 14) to P, λ is the wavelength of the radiation, and the exponential gives the phase delay due to the covered distance r.

Being $r \to \infty$, we can write $\overline{OP} = R \simeq \overline{HP}$ and thus:

$$r = R + x\sin\varphi \simeq R + x\varphi \tag{1.14}$$

Eq. (1.13) thus becomes:

$$dE = g(x)\mathrm{e}^{-2\pi i R/\lambda} e^{-2\pi i(x/\lambda)\sin\varphi} dx \tag{1.15}$$

If we integrate over the whole size of the aperture, we get:

$$E = e^{-2\pi i R/\lambda} \int g(x)\mathrm{e}^{-2\pi i(x/\lambda)\sin\varphi} dx \tag{1.16}$$

Since $\left|e^{-2\pi i R/\lambda}\right| = 1$ we can neglect this term in the following analysis. It only repents a constant that can always be considered equal to one[5]. Since out of the aperture $g(x) = 0$, we can integrate Eq. (1.15) from $-\infty$ to $+\infty$. Eq. (1.16) then becomes:

$$E(\varphi) = e^{-2\pi i R/\lambda} \int_{-\infty}^{+\infty} g(x)\mathrm{e}^{-2\pi i(x/\lambda)\sin\varphi} dx \propto \int_{-\infty}^{+\infty} g(u)\mathrm{e}^{-2\pi i u s} du \tag{1.17}$$

where $u = x/\lambda$ and $s = \sin\varphi$.

Eq. (1.17) shows that *the electric field in a generic point P of the image screen (Fraunhofer plane) is given by the Fourier Transform (F.T.) of the grading*. This electric field is a feature of the adopted optical system (e.g. slit, antenna, grating, ...). This is a generic result. $E(\varphi)$ is known as *field radiation pattern* (or *angular spectrum of the radiation*, the word spectrum being related to the Fourier analysis).

The image at infinite distance, that is the power measured by a receiver, is $\propto \left|E(\varphi)\right|^2$. If the incoming wave is plane, such as the wave emitted by a point source at infinite distance, the image gives directly the diffraction pattern of the instrument. In the astronomical case, the image screen is usually located in the focus of a convergent system (lens, parabolic mirror), but the main results of what we have shown do not change.

We will now examine some typical cases. In the following, all the lengths will be measured in units of wavelength (i.e. $x(m)/\lambda(m)$).

5 When R is an integer multiple of λ.

In the case of an *aperture (slit) of width* u traversed by a plane wave, the grating is given by the *rectangle function*[6] *(Fig. 16)*:

$$g(x) \propto \prod(x/u) \tag{1.18}$$

that is:

$$g(x) \neq 0 \Leftrightarrow |x| < u/2$$

We know that the F.T. of the rectangle function is the *sinc* function (Fig. 17). The field radiation pattern is therefore given by:

$$\boldsymbol{E(\varphi) \propto sinc(u \sin\varphi) = \frac{\sin(\pi u \sin\varphi)}{\pi u \sin\varphi} = \frac{\sin\psi/2}{\psi/2}} \tag{1.19}$$

where $\psi = 2\pi u \sin\varphi$. In this case, t*he electric field is the sum of an infinite number of sinusoids whose frequencies variate continuously between 0 and* $u/2$. The intensity of the diffraction image as a function of φ is given by the function $sinc^2$, characterized by a strong principal maximum and secondary maxima with decreasing intensity (see Fig. 18). **The first zero of the electric field is found for** $\boldsymbol{\pi u \sin\varphi = \pi \rightarrow \varphi \approx \sin\varphi = 1/u}$. The width of the principal maximum therefore decreases with increasing u (i.e. the width of the aperture in units of wavelength).

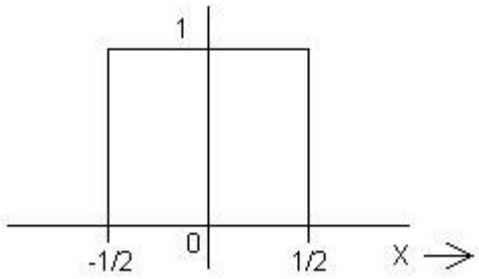


Figure 16: Rectangle function

6 Note that the variable x/u is dimensionless.

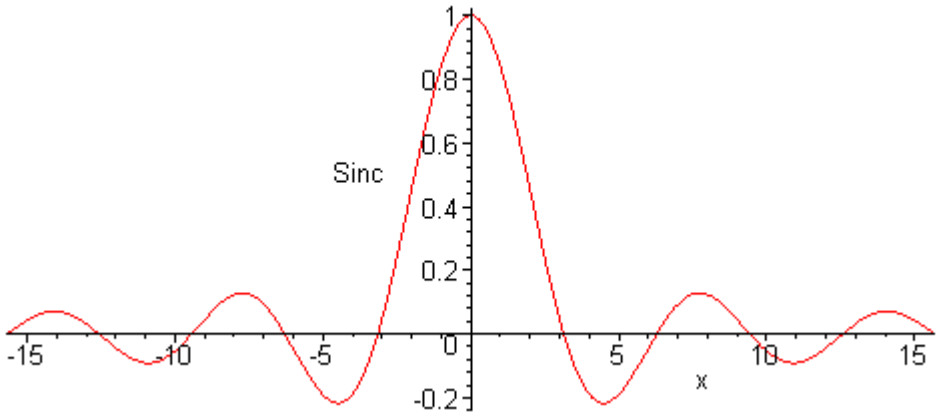


Figure 17: sinc function

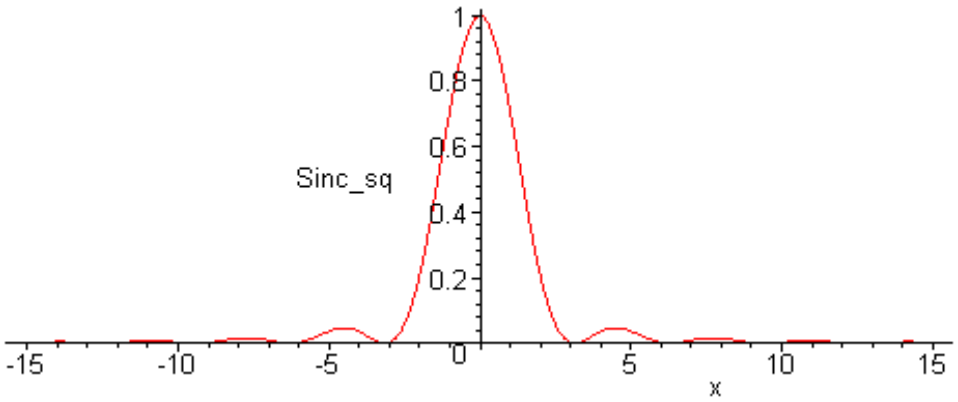


Figure 18: sinc square function

Consider now a system made up of *two equal apertures* (antennae) *located at a distance* $\pm u$ *from the origin of the reference system* (i.e. an *interferometer*). The total electric field is given by:

$$g(x)=g_0(x)*[\delta(x-u/2)+\delta(x+u/2)] \qquad F.T.[g_0(x)]=E_0(\varphi) \tag{1.20}$$

where $g_0(x)$ is the grading of each antenna, δ is the Dirac delta function and $*$ indicate the convolution operation. If we apply the convolution theorem ($F.T.(f(x)*g(x))=F(u)\times G(u)$, where $F.T.(f(x))[(g(x))]=F(u)[G(u)]$), we get:

$$\boldsymbol{E(\varphi)=2\,E_0(\varphi)\cos(\pi u\sin\varphi)=2\,E_0(\varphi)\cos\psi/2} \tag{1.21}$$

(again $\psi = 2\pi u \sin\varphi$) since:

$$F.T.(g_0(x)) = E_0(\varphi)$$
$$F.T.(\delta(x-u/2)+\delta(x+u/2)) = 2\cos(\pi u \sin\varphi)$$

where $u\sin\varphi$ is the phase difference of the signals arriving on the two antennae, due to the geometric delay τ , as shown in Fig. 19.

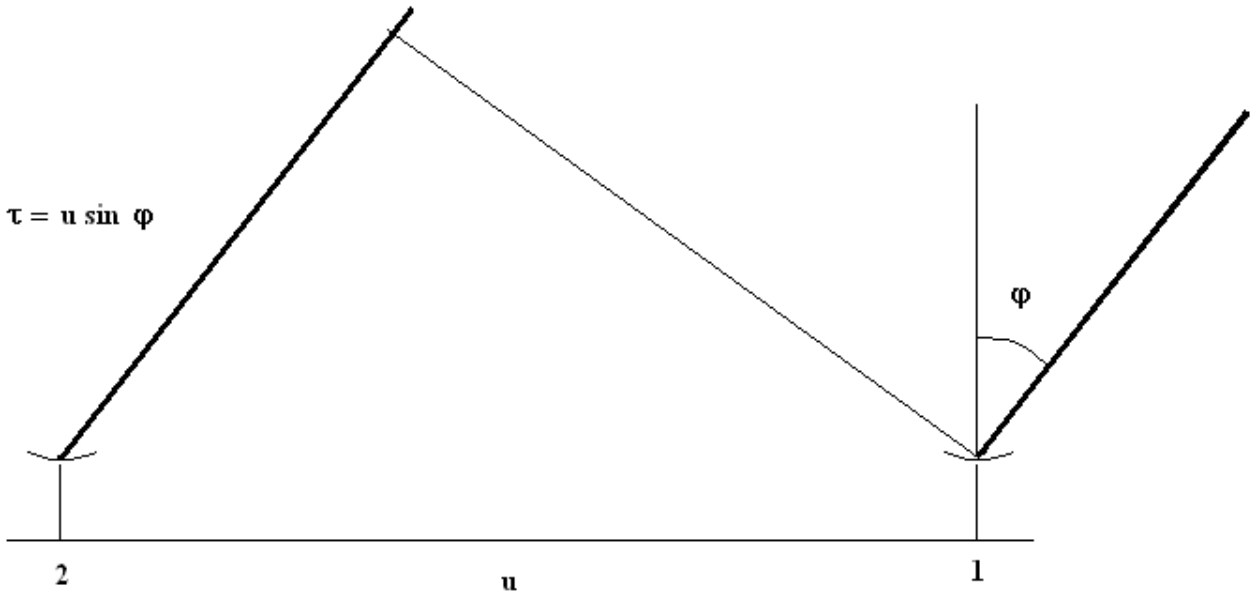


Figure 19: Pattern of the two antennae interferometer

Its is very important to stress that in such a case the field radiation pattern related to the interference coming from the two antennae is given by a single (co)sinusoid, and it is therefore characterized by a single spatial frequency ($u/2$ in units of λ). The pattern of $|E(\varphi)|^2$ is shown in the bottom panel of Fig. 20. The rapid oscillations are due to the interference coming from the two antennae (middle panel of Fig. 20), while the modulation is due to the diffraction pattern of each single antenna (top panel of Fig. 20 and Fig. 18).

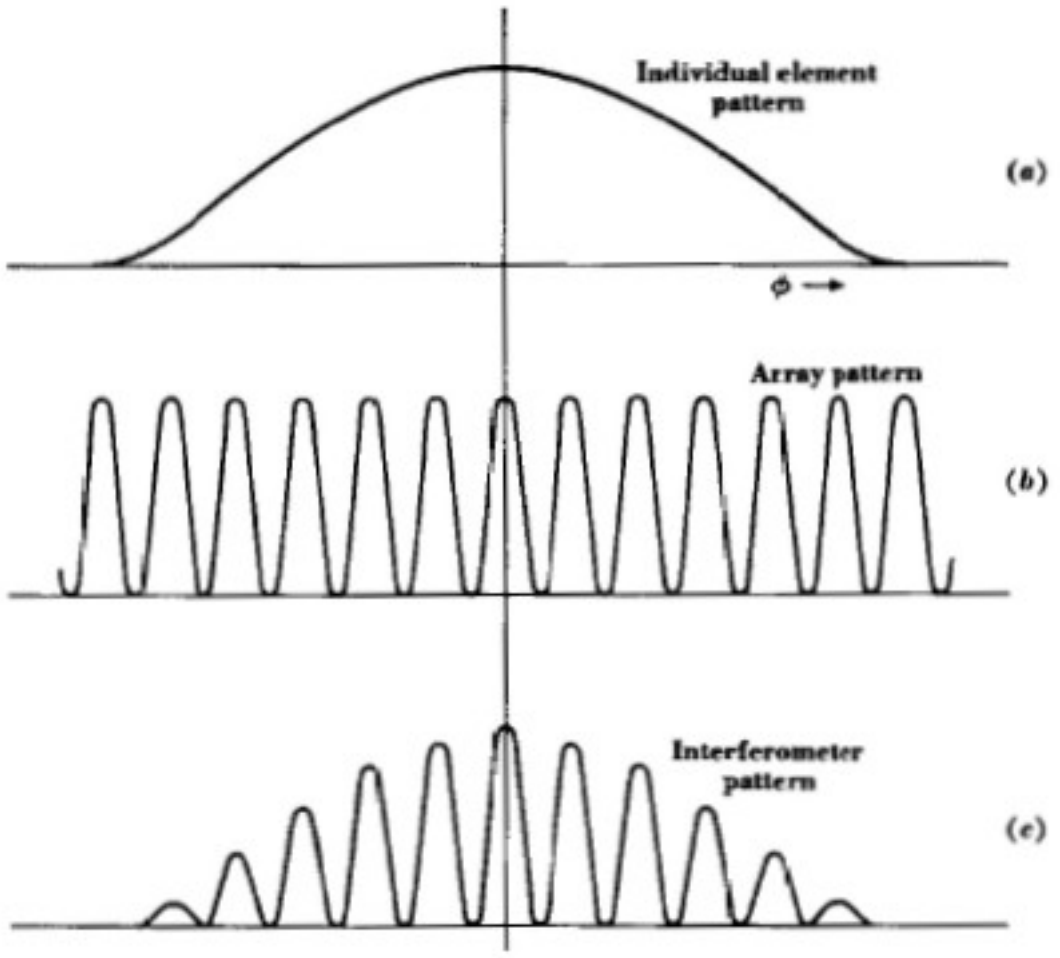


Figure 20: Power pattern for a uniformly illuminated aperture (top), for a two-beam interferometer (middle) and for a two-antenna interferometer (bottom)

From Eq. (1.21), in such a case **the first zero is found for** $\pi u \sin\varphi = \pi/2 \rightarrow \varphi \approx \sin\varphi = 1/2u$. Eq. (1.21) also shows that $|E(\varphi)|^2$ is maximum when $\psi/2 = \pi u \sin\varphi = k\pi, k = 0,1,2,\ldots$, while it is null when $\psi/2 = \pi u \sin\varphi = (2k+1)\pi/2, k = 0,1,2,\ldots$. The distance between two successive maxima is therefore given by $\Delta(\sin\varphi) = 1/u$ (since: $\psi_1/2 = k\pi$, $\psi_2/2 = (k+1)\pi$, $\Delta\psi = 2k\pi + 2\pi - 2k\pi = 2\pi$; thus: $2\pi u \Delta(\sin\varphi) = 2\pi \rightarrow \Delta(\sin\varphi) = 1/u$).

In a similar way, we can show that, in the case of a *multiple interferometer made up by N equidistant* (*d* being the distance in units of λ) *antennae (i.e. a grating),* the field radiation pattern $E(\varphi)$ is given by:

$$\boldsymbol{E(\varphi)=E_0(\varphi)\frac{\sin N\psi/2}{\sin\psi/2}} \tag{1.22}$$

where $\psi=2\pi d\sin\varphi$ and $E_0(\varphi)$ is the radiation pattern of each single antenna. Of course, for $N = 2$ Eq. (1.22) corresponds to Eq. (1.21):

$$E(\varphi)=E_0(\varphi)\frac{\sin\psi}{\sin\psi/2}=E_0(\varphi)\frac{2\cos\psi/2\sin\psi/2}{\sin\psi/2}=2E_0(\varphi)\cos\psi/2$$

The sine function at the numerator of Eq. (1.22) has a period that is N times lower compared to the sine function at the denominator. Therefore the zeros of $E(\varphi)$ are essentially determined by the number of antennae of the interferometer. **We find the first zero for:**

$$\boldsymbol{N\psi/2=\pi\rightarrow N\frac{2\pi d\sin\varphi}{2}=\pi\rightarrow\varphi\sim\sin\varphi=\frac{1}{Nd}}$$

Eq. (1.22) never diverges, since $\sin\psi/2=0$ when also $\sin N\psi/2=0$, and its principal maximum (corresponding to the *main lobe* in Fig. 21) is given by $N E_0(\varphi)$. The secondary maxima (also called *maxima of grating* and corresponding to the *grating lobes* in Fig. 21) dist $1/d\cos\bar{\varphi}$ from each other, $\bar{\varphi}$ being the mean direction of the N antennae with respect to the grating axis. Their value would also be $N E_0(\varphi)$ if they would not be modulated by the field radiation pattern of the single antenna $E_0(\varphi)$ (see Fig. 21).

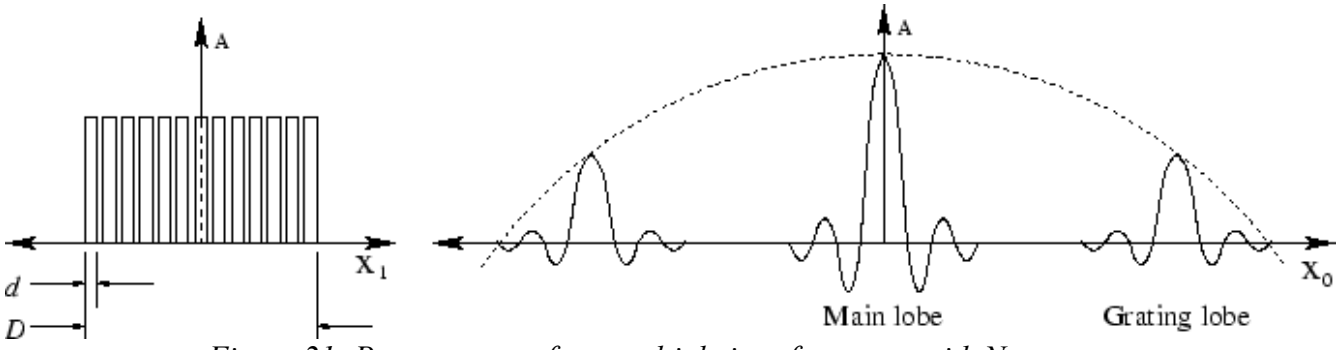


Figure 21: Power pattern for a multiple interferometer with N antennae

The diffraction figure is basically characterized by two parameters: its resolving power (or angular/spatial resolution) and the height of secondary maxima. An instrument's angular resolution refers to how well it can distinguish between two objects in space which are separated by a small angular distance - it is the telescopes ability to resolve fine detail. The closer two objects can be while still seen as two separate objects, the higher the spatial resolution of the telescope. The spatial resolution of a telescope affects how well details can be seen in an image. A telescope with higher spatial resolution creates more detailed images (see for instance Figs.22, 23, 24).



Figure 22: Mean...



Figure 23: ...and high resolution image of M31

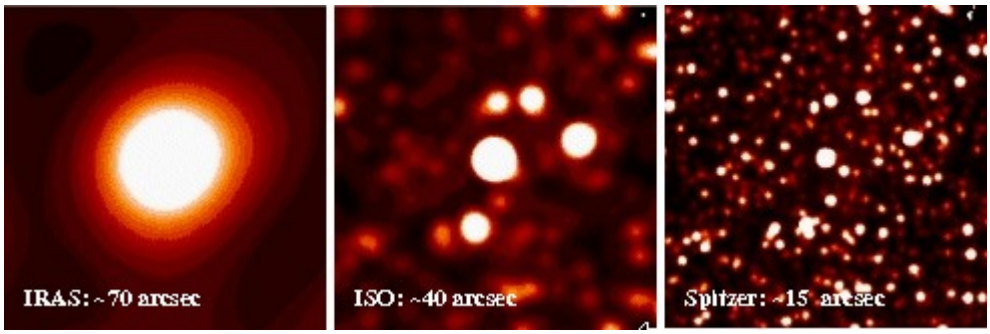


Figure 24: Influence of angular resolution on FIR (160 microns) observations

In order to characterize the resolving power of an instrument, generally either the full width at half maximum (FWHM) or the distance between the first two zeros are given. The latter have been estimated in the case of the three kind of instruments considered above:

single aperture: $2/u$

2 antennae interferometer: $1/u$

N antennae interferometer: $2/Nd = 2/u$

where u indicates the total size of the instrument. We thus observe that, for a given u, the simple interferometer (with only 2 antennae) has a resolving power that is twice better than the other two instrument configurations.

The quality of an image, however, depends also on the diffraction image of the telescope, since high grating lobes can significantly compromise the observations and all the chain of operations to treat them (restoration). This is particularly true in the case of observations of extended radio sources. Actually, a binary system consisting of two unresolved point sources produces a pattern resulting from the superposition of two individual point sources shifted relative to each other by their angular separation. These two sources can thus be resolved if the separation of the two sources is larger than the width of the main beam (i.e. the main lobe). Two point sources, respectively resolved and not resolved, are shown in Fig. 25 (last two cases from left to right). In the case of extended sources, interferometers (with 2 or more antennae) can give more problems compared to a filled aperture. This is due to the fact that, as we can see by comparing Figs. 18, 20 and 21, despite its better angular

resolution, the simple interferometer is characterized by the highest secondary maxima, which decrease in the case of the multiple interferometer and, even more, in the case of the single aperture configuration. The filled aperture produces an image of an extended source that is a smoothed version of the true distribution (first case in Fig. 25), where the smoothing is produced by the finite angular size of the main and grating lobes. Provided the grating lobe is small this will be a reasonably accurate and only slightly smoothed version of the true distribution. For the two (or *N*) elements interferometer, the situation is different due to their significantly higher grating lobes. If the source extends beyonds the first of them, the radiation received by the grating lobes will be combined with that from the main beam, and the resulting image will be a greatly distorted version of the true image (see Fig. 26). We will see in the next chapters how we can manage to solve, at least in part, this problem.

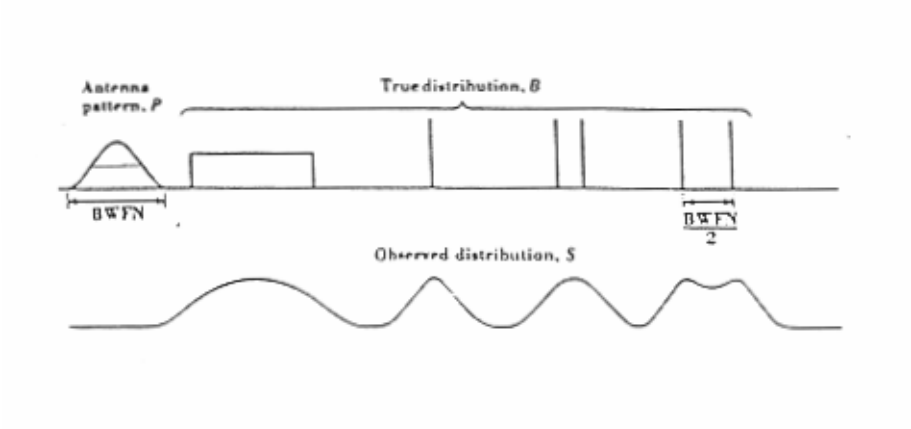


Figure 25: Smoothed distribution S observed with an antenna pattern P

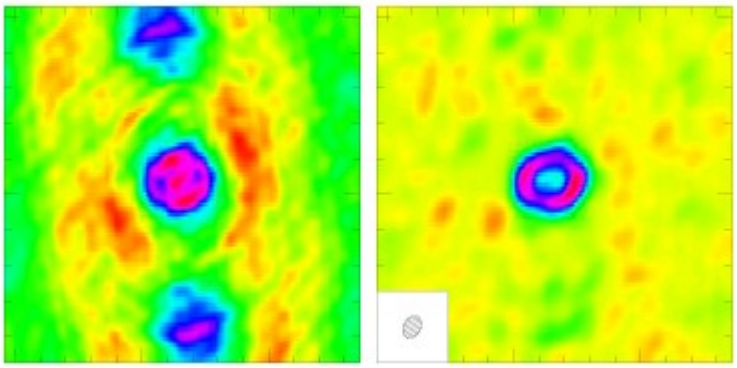


Figure 26: Dirty and clean image of an extended source

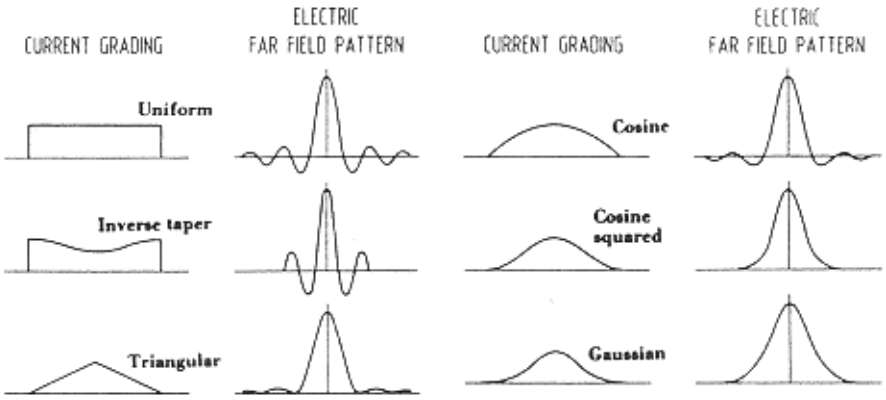


Fig. 6.2. Pairs of current gradings and corresponding electric far field pattern.

Figure 27: Different aperture distributions with associated field patterns

In Fig. 27, the power pattern for different aperture distributions (i.e. telescope configurations) are shown. For the same value of u, the softest gradings have field pattern with a worst resolving power, but lower grating lobes (if any, as in the case of the cosine squared or the Gaussian grading). This property is largely exploited in radio observations. By applying a *taper* (i.e. a grading with a lower amplitude at the borders than at the center) we can significantly reduce the grating lobes, despite a loss in resolution. An i*nverse taper* can also be used with the opposite purpose ("increasing" the angular resolution[7], even if augmenting the grating lobe amplitude). We have therefore to remember that *the resolving power of an instrument does not depend only on its size (in units of wavelengths), but also on the distribution of the spatial frequencies covered by the telescope and on their relative weight*.

Let's conclude this part of the lecture by seeing what the diffraction pattern of an instrument means in practice. In signal processing the *impulse response* of a system is its output signal in response to an impulse signal (Dirac delta function). In the cases seen above, the impulse response is given by the diffraction pattern. Given the sky brightness $B(\varphi)$, and $P(\varphi)=|E(\varphi)|^2$ being the diffraction pattern of the system, we can write the observed brightness at a position φ_0 as:

7 Note that, when we say "increase the angular resolution", we mean to make its value lower. In other words, "increase" stand for "improve".

$$B_0(\varphi_0)=\int_{-\infty}^{+\infty} B(\varphi)P(\varphi_{0,}\varphi)d\varphi \tag{1.23}$$

If the diffraction pattern is space independent:

$$B_0(\varphi_0)=\int_{-\infty}^{+\infty} B(\varphi)P(\varphi_0-\varphi)d\varphi \tag{1.24}$$

Based on the autocorrelation theorem ($F.T.(f^{\star}(x)\odot f(x))=|F(u)|^2$, where $\odot$ indicates the auto-correlation operation) and on Eq. (1.17) ($F.T.(g(x))=E(\varphi)$) we can write:

$$P(\varphi)=|E(\varphi)|^2=F.T.(g(x)\odot g(x)) \tag{1.25}$$

$P(\varphi)=|E(\varphi)|^2$ is thus the F.T. of the autocorrelation function of the grading ($g(x)\odot g(x)$). Since the F.T. of the impulse response of an interferometer is the so called *transfer function* of an instrument, for what said above we can state that *the autocorrelation function of the grading* $g(x)\odot g(x)$ *represents the transfer function of the system*, i.e. the mathematical representation of the relation between the input and output of the instrument.

In the case of a filled aperture of width u (represented by a rectangle function), for example, we will have:

grating : $g(x)\propto\prod(x/u)$ (rectangle function)

impulse response : $P(\varphi)=|E(\varphi)|^2\propto sinc^2(u\sin\varphi)$ (sinc square function)

transfer function : $g(x)\odot g(x)\propto\wedge(x/u)$ (triangle function)

Note that, as it has to be, F.T. $F.T.(\wedge(x/a))=a\,sinc^2(ua)$. To conclude, if we know the transfer function of an instrument we can immediately estimate the diffraction pattern (and thus the resolving power) of an instrument and *vice versa*.

1.5 The radio telescope: hints to its basic properties

As an optical telescope, the radio telescope is made up by tow main parts: one that collects the incoming e.m. radiation and conveys it to the sensor (*antenna*), the other that is able to reveal the signal (*receiver*). Therefore the antenna has the same role played by the mirror in an optical telescope, the receiver corresponds to the photographic plate (in former times) or to the CCD (at present).

The antenna is a device which is able to transform the incoming e.m. energy into a measurable electric tension. The most simple antenna is a *dipole*, i.e. a metallic bar whose transversal dimension is negligible when compared to its length. Usually the length of the adopted dipole is equal to the observed wavelength (or half of it). In such a case we are in resonance conditions and the signal reception is better. More generally, the antenna is a metallic, often discontinuous surface (*mirror*) that has the main function to collect the e.m. radiation and convey it to the receiver device (*feed*). The mirror can be built following different schemes (e.g. *equatorial (polar)* mount - the structure is driven about one axis (the *polar axis*) that is parallel to the Earth's rotation axis and about an orthogonal axis (the *declination axis*); Fig. 28 - or *altitude-azimuth* - the antenna is driven in altitude by rotating it around a horizontal axis (elevation axis) and in azimuth by rotating it around a vertical axis (azimuth axis). The aperture rotates with respect to the sky as the antenna tracks a celestial source; Fig. 29). The "mirror" can also be made up by distinct elements (antennae), often far away from each other, but working simultaneously (*interferometers*).

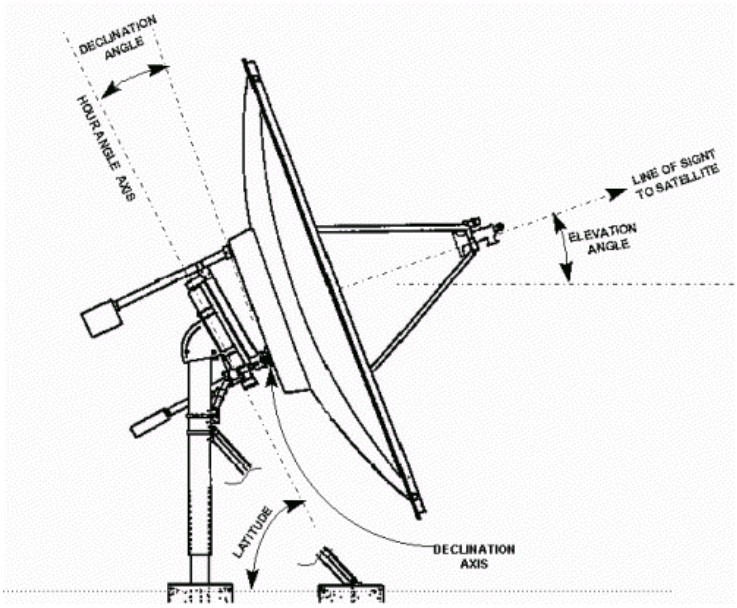


Figure 28: Example of equatorial (polar) mount

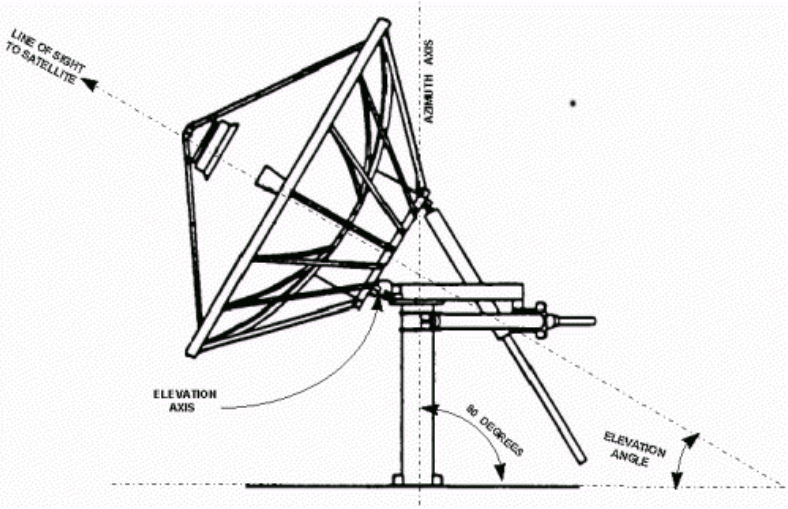


Figure 29: Example of altitude-azimuth mount

Has we have previously pointed out, a radio telescope, as all the other kinds of instruments, is characterized by its ***diffraction pattern***, or ***antenna diagram***, or ***power pattern*** or ***beam***. In different words, the presence of a beam means that an antenna radiates different amounts of power in different directions. The shape of the power pattern depends on both spherical coordinates θ and φ . Quite often the ***normalized power pattern*** (and not the power pattern) is given:

$$P_n(\theta,\varphi)=\frac{P(\theta,\varphi)}{P_{max}(\theta,\varphi)} \tag{1.26}$$

The *beam solid angle* Ω_A of an antenna is given by:

$$\Omega_A=\iint_{4\pi} P_n(\theta,\varphi)\,d\,\Omega=\int_0^{2\pi}\int_0^{\pi} P_n(\theta,\varphi)\sin\theta\,d\,\theta\,d\,\varphi \quad \text{(sr)} \tag{1.27}$$

The integration is extended over the full sphere 4π , such that Ω_A is the solid angle of an ideal antenna having $P_n=1$ inside Ω_A , $P_n=0$ everywhere else. Actually, such an antenna does not exist since real antennae have normalized power patterns with considerably larger values for a certain range of θ and φ than for the rest of the sphere. The strongest maximum of the diffraction pattern is called *main lobe* or *main beam* of the antenna, while secondary maxima are called *side lobes* or *back lobes* (see Fig. 30). The angular extent of the main beam is generally described by the *half*

power beam width (HPBW – the angle between points of the main beam where the normalized power pattern falls to ½ of the maximum). Other possible definitions always related to the resolution of the instrument and therefore the width of the main lobe are: *full width to half power* (FWHP – equivalent to HPBW), *beam width between first nulls* (BWFN) or *equivalent width of the main beam* (EWMB). For main beams with non circular cross sections, values for widths in orthogonal directions are needed.

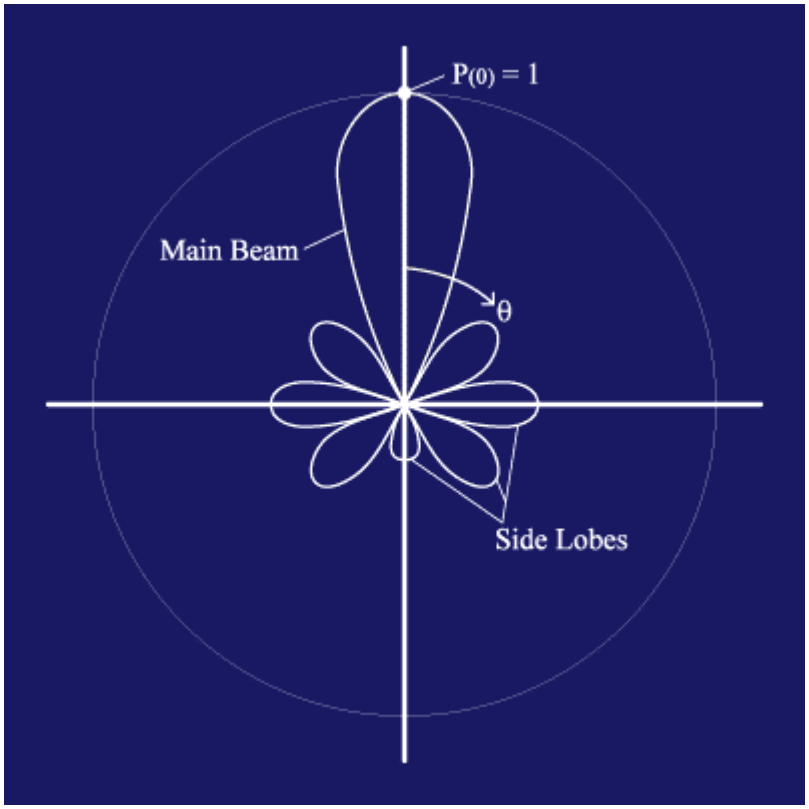


Figure 30: Example of a two-dimensional representation of a hypothetical power pattern

In analogy to Eq. (1.27) we can also define the *main beam solid angle* Ω_{MB} :

$$\Omega_{MB} = \iint_{main-lobe} P_n(\theta,\varphi)\, d\Omega \quad \text{(sr)} \tag{1.28}$$

As we have said before, in order to have good quality images, we need low secondary maxima in the diffraction pattern of the instrument. We can add that the quality of an antenna as a direction measuring device depends on how well the power pattern is concentrated in the main beam. It is thus

appropriated to define a *main beam efficiency* (or simply *beam efficiency*), η_B , by:

$$\eta_B = \frac{\Omega_{MB}}{\Omega_A} \tag{1.29}$$

It is important to stress that η_B has nothing to do with the angular size of the main beam, since it only indicates how much of the power pattern is concentrated in the main beam. As we have seen before (e.g. Fig. 27), the main beam efficiency can be modified by changing the distribution of the spatial frequencies covered by the telescope and their relative weight (for example by a choice of feed systems which provide the appropriate illumination of the dish).

An antenna is also characterized by its ***directivity***:

$$D = \frac{4\pi}{\Omega_A} \tag{1.30}$$

and by its **e*ffective aperture***, defined as the ratio between the measured power and the flux (known) of a calibration source. It is therefore a measure of the power extracted by the antenna from the incoming plane wave, and it is given by:

$$A_e = \frac{w(\theta,\varphi)}{S} \quad (\mathrm{m}^2) \tag{1.31}$$

where $w(\theta,\varphi)$ is the power measured by the antenna and *S* is the true flux of the source. The aperture efficiency of an antenna (η_A) is defined as the ratio between its effective and *geometric aperture* A_g :

$$\eta_A = \frac{A_e}{A_g} \tag{1.32}$$

It can be shown[8] that the effective aperture of an antenna and its directivity are related by:

8 For a clear demonstration , not in the purpose of this introductory lecture, see "Tools of Radioastronomy" by K. Rholfs and T. Wilson, Springer Ed.

$$D = \frac{4\pi A_e}{\lambda^2} \tag{1.33}$$

and thus, combining Eqs. (1.30) and (1.33), we get:

$$A_e \Omega_A = \lambda^2 \tag{1.34}$$

Another important concept to be introduced when studying radio telescopes is the ***antenna temperature***. Consider a receiving antenna with a normalized power pattern $P_n(\theta, \varphi)$, receiving e.m. radiation from a source characterized by a (monochromatic) brightness distribution $B_\nu(\theta, \varphi)$. Based on Eqs. (1.2) and (1.31), the antenna will deliver at its output terminals a total power per unit bandwidth of:

$$w = m A_e \iint B_\nu(\theta, \varphi) P_n(\theta, \varphi) d\Omega \tag{1.35}$$

where the factor *m* takes into account the fact that the incoming e.m. radiation is usually not polarized, or only partially polarized. Since antennae are able to receive only one component of polarization, only a fraction of the radiation will be detected. In the most common case of non-polarized radiation $m = 1/2$ (see Figs. 10, 11, 12 and relative discussion). Using the Nyquist formula ($P = kT$), we can introduce an *equivalent antenna temperature* given by:

$$w = k T_A \tag{1.36}$$

where $k = 1.38 \times 10^{-23} Joule/°K$ is the Boltzmann constant. This definition of antenna temperature relates the output of the antenna to the power of a matched resistor. When these two power levels are equal, then the antenna temperature is given by the temperature of the resistor.

We can now *relate the antenna temperature* T_A *and the brightness temperature* T_b *concepts*. By combining Eqs. (1.35), (1.36) and (1.34) we get:

$$T_A(\theta,\varphi)=\frac{w}{k}=m\frac{A_e}{k}\iint B_\nu(\theta,\varphi)P_n(\theta,\varphi)\,d\Omega=m\frac{\lambda^2}{k\,\Omega_A}\iint B_\nu(\theta,\varphi)P_n(\theta,\varphi)\,d\Omega \qquad (1.37)$$

Since $T_b=\frac{c^2}{2k}\frac{1}{\nu^2}B_\nu$ (Eq. (1.10)) and remembering that $\lambda=\frac{c}{\nu}$, Eq. (1.37) becomes:

$$T_A(\theta,\varphi)=\frac{2m}{\Omega_A}\iint T_b(\theta,\varphi)P_n(\theta,\varphi)\,d\Omega \qquad (1.38)$$

(where, as said, in most of the cases $2m \sim 1$), which, combined with Eq. (1.27), gives:

$$\boldsymbol{T_A(\theta,\varphi)=\frac{2m\iint T_b(\theta,\varphi)\,P_n(\theta,\varphi)\,d\Omega}{\iint P_n(\theta,\varphi)\,d\Omega}} \qquad (1.39)$$

Since, based on their definitions, T_A is the quantity that we measure, while T_b is the one desired, Eq. (1.39) must be inverted . It is an integral equation of the first kind, which in theory can be solved if $T_A(\theta,\varphi)$ and $P_n(\theta,\varphi)$ are known. In practice this inversion is possible only approximately. As we will see in more details in the following, usually $T_A(\theta,\varphi)$ and $P_n(\theta,\varphi)$ are known only for a limited range of θ and φ values, and the measured data are affected by errors. Therefore an approximated deconvolution of Eq. (1.39) is only possible.

A final and important note concerning Eq. (1.35). If the integral is extended over all the source, the quantity:

$$S=\iint_{source} B(\theta,\varphi)P_n(\theta,\varphi)\,d\Omega \qquad (1.40)$$

do not correspond to the total flux of the radio source $S_\nu=\int_{source} B_\nu(\theta,\phi)\,d\Omega$ (Eq. (1.5)). This is true only if the radio source has a very small angular size compared to the antenna pattern. In such a case $P_n(\theta,\varphi)\approx 1$, and Eqs. (1.5) and (1.40) coincide. If the brightness distribution is instead more extended than the beam, we need to point the antenna towards different sky positions φ_0 in order to

cover the whole object. For each pointing we will measure:

$$\boldsymbol{S(\varphi_0)=\int_{beam} B(\varphi)P_n(\varphi_0-\varphi)\,d\varphi} \tag{1.41}$$

This is called ***flux per beam area*** and it is *analogous to a brightness*, as it represents the spectral power received per unit area and per unit solid angle. For the latter the units is the beam instead of sr. Also in this case we speak about *observed brightness*.

In order to get the total observed flux, we integrate Eq. (1.41) in φ_0 . If the brightness of the object does not variate significantly over the beam extension ($B(\varphi)\approx B(\varphi_0)=const.$), we have:

$$S_{obs}=\int_{source} d\varphi_0 \int_{beam} B(\varphi)P_n(\varphi_0-\varphi)\,d\varphi \approx \int_{source} B(\varphi_0)\,d\varphi_0 \int_{beam} P_n(\varphi_0-\varphi)\,d\varphi \tag{1.42}$$

and thus, from Eq. (1.27) and (1.5):

$$\boldsymbol{S_{obs}\approx \Omega_A S} \tag{1.42}$$

that means that ***the flux of the radio source can be obtained, as a first approximation, as the ratio between the observed flux and the beam area.***

If we combine Eqs. (1.32), (1.35), (1.36) and (1.40) we get:

$$S=\frac{k\,T_A}{m\,A_e}\propto\frac{k\,T_A}{\eta_A A_G}=\frac{T_A}{\boldsymbol{G}} \tag{1.43}$$

where the ***antenna gain*** is give by the quantity $\boldsymbol{G=\frac{\eta_A A_G}{k}}$ (°K/Jy). As the effective aperture, the antenna gain measure the capability of an antenna to collect the flux *S*. For the same value of a source flux S , the higher is G , the higher is T_A , making the signal detection easier. The antenna gain is one of the different parameters that we need to do observations of radioastronomical sources. Let's

see why.

As we have said, a radio telescope is made up by a sensor that conveys the signal from a source into a receiver. If the sensor is a paraboloid, the receiver is made up by a feed directly connected by cables to the antenna. For different antenna's shape (e.g. cylinders, T, distinct elements...) we have different feeds that can be connected each other basically in two way: the single signals are either added or multiplied. In most of radio telescopes the second solution is adopted. In these lectures we will not enter in more details about this, but one important thing to know about receivers is that they are affected by different sources of system noise. Besides the receiver in itself and the radiation coming from the sky object we want to observe, the atmosphere, the spillover noise of the antenna[9], the noise produced in the guides and cables connecting the feed to the receiver input all contribute to the total receiver power. All these contributions are additive and are given by the *system temperature*:

$$T_{sys} = \sum T_i \tag{1.44}$$

where T_i is the noise temperature of the individual contributors listed above. In particular, we can write the system temperature as:

$$T_{sys} = T_A + T_R \tag{1.45}$$

where T_A is associated to the signal coming from the astronomical source, T_R to all the sources of noise associated to the receiver. In general T_A is negligible compared to T_R and thus we can write that $T_{sys} \approx T_R$. How is it possible, then, to make radio astronomical observations? For this we do not need that the flux we have to measure is higher than the spurious signal coming from the receiver. As schematically shown in Fig. 31, t**he flux to be observed has to be *n* times (*n* = 3 or 5) higher than the noise associated to** $T_{sys} \approx T_R$ **.**

We have now to understand how we can derive the noise of an instrument. During observations we are usually interested in measuring fluxes in narrow frequency bands, in order to have nearly

9 It consists of ground radiation that enters into the system through far side lobes.

monochromatic radiation. If we indicate with $\Delta\nu$ the observed bandwidth, from Fourier Transform theory we know that the time resolution Δt for independent samples is given by $\Delta\nu\Delta t=1$. This means that two samples taken at time interval less than $\Delta t=1/\Delta\nu$ apart are not independent. An observation lasting a total time τ contains thus $N=\tau/\Delta t=\tau\Delta\nu$ independent samples. Gaussian statistics shows that the total error for N samples is $1/\sqrt{N}$ of that of a single sample. Assuming that the error on the single sample is αT_{sys} with $\alpha\simeq 1$, we can therefore write the mean quadratic error associated to a radioastronomical measure as:

$$\Delta T_{r.m.s.}=\frac{\alpha T_{sys}}{\sqrt{\Delta\nu\tau}} \tag{1.46}$$

where $\Delta\nu$ is the receiver bandwidth and τ is the total integration time of the observations. By combining Eqs. (1.46) and (1.43) we can thus write:

$$\Delta S_{r.m.s.}=\frac{\Delta T_{r.m.s.}}{G}=\frac{\alpha(T_A+T_R)}{G\sqrt{\Delta\nu\tau}}\approx\frac{\alpha T_R}{G\sqrt{\Delta\nu\tau}} \tag{1.47}$$

(remember that T_A <<< T_R). As we have seen above, if the source of the flux is about 5 times the noise of the instrument the observation is adequate, i.e. it has to be:

$$S_{source}>5\times\Delta S_{r.m.s.}\approx\frac{5\alpha T_R}{G\sqrt{\Delta\nu\tau}} \tag{1.48}$$

In the previous equations the parameters α , T_R , G and $\Delta\nu$ depend on the telescope. The only quantity that we can variate is the total integration time (i.e. the total time of the observations), since, by increasing it, we reduce $\Delta S_{r.m.s.}$ thus increasing the *signal to noise ratio*:

$$S/N=S_{source}/\Delta S_{r.m.s.} \tag{1.49}$$

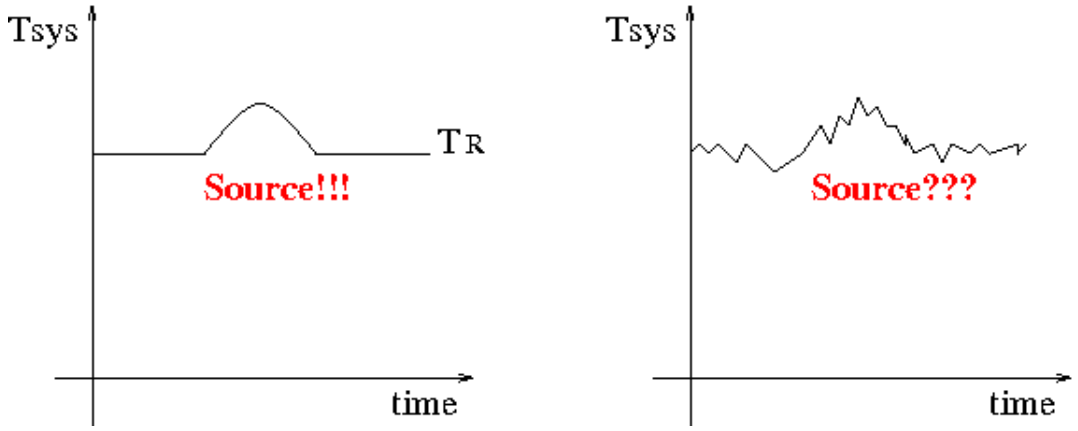


Figure 31: Source detection in a noiseless (left) and very noisy (right) observation

1.6 The need of resolution: some basic concepts about interferometry

In the previous chapters, using diffraction theory we have shown that a) the sensitivity of the radio telescope is proportional to the area of the antenna used to collect incoming radiation (effective aperture concept), and b) the resolution of a radio telescope is $\delta \sim \lambda / D$, where δ is the smallest angular separation which two point sources can have in order to be recognized as separate objects, λ is the wavelength of the radiation received, and D is the diameter of the telescope (see Fig.31).

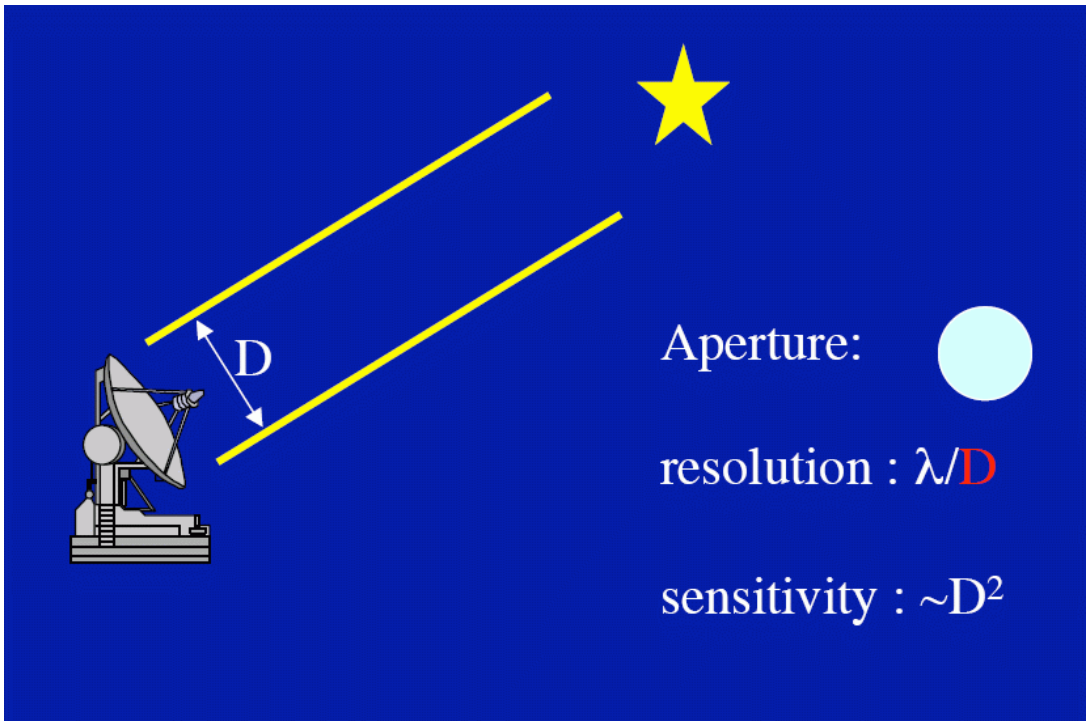


Figure 32: Sensitivity and resolution of a single antenna

In order to improve the angular resolution, for a given wavelength, the diameter D of the telescope must be increased. Materials, however, limit the size of a single telescope to ~ 300 m.

We halve also seen that a resolving power of order $\delta = \lambda / B$ can be obtained by coherently linking two small telescopes separated by a certain distance (*interferometer*). We will call B (***baseline***) the component of the distance between the two antennae in a direction perpendicular to the incoming radiation (Fig. 33). We have seen that interferometers can give however serious problems in imaging astronomical sources due to the presence of high side lobe levels in their diffraction pattern.

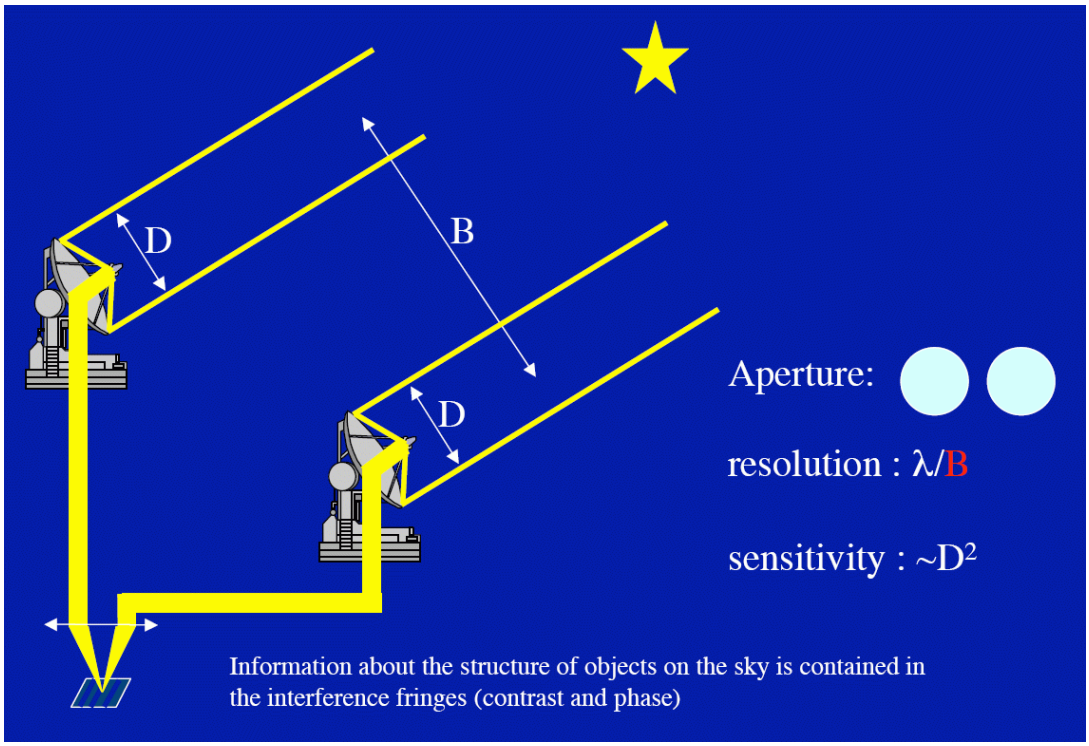


Figure 33: Sensitivity and resolution of an interferometer (with two antennae)

In the following, we will see some basic concepts about radio interferometry, without entering in any details, but trying to understand how we can get a proper image of astronomical radio sources using interferometry and exploiting its incredibly good angular resolution (see Fig. 34). This text is therefore not complete at all for all what concerns interferometry and the related topics.

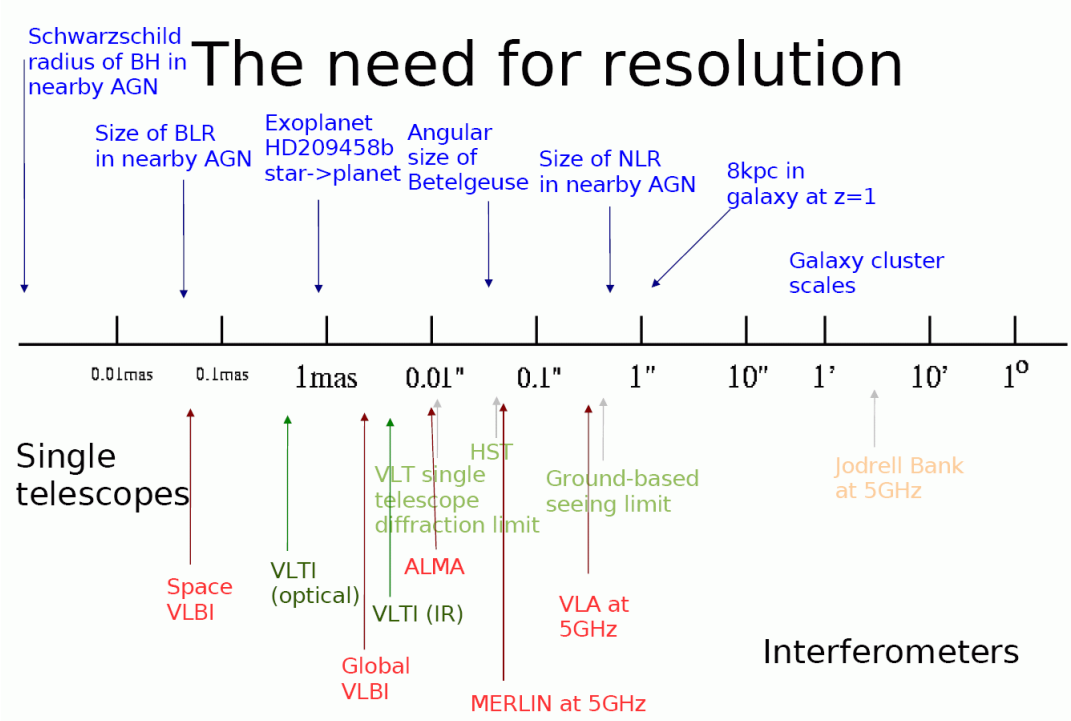


Figure 34: Comparison of the angular resolution of different single telescopes and interferometers. In the upper part of the image the angular size of different kind of astronomical sources is shown

We have seen before that the power received from a source offset by angle $\Theta=(\theta,\varphi)$ from the pointing direction is not its "true" brightness, but it is reduced by the beam of the instrument. We can say that, due to its diffraction pattern the antenna responds to a *modified sky brightness function* $I'(\Theta)=A(\Theta)I(\Theta)$, that means that $I'(\Theta)$ is the intensity of the object $I(\Theta)$ as modified by the beam shape $A(\Theta)$.

In the case of a double interferometer, its output is formed by multiplying together (correlating) the voltages received by the two antennas, and integrating. An interferometer stationary in space, observing a non-variable source, can produce two independent numbers, known as the cosine and sine outputs. They are also commonly considered to be the real and imaginary components of a quantity called the ***complex visibility***, or just the *visibility*, V. It exists a theorem (the van Citter-Zernike theorem)[10] which states that *the visibility* V *is the F.T. of the modified sky brightness function* $I'(\Theta)$ *:*

10 If you want more details see, for instance, "Interferometry and Synthesis in Radio Astronomy" by R.A. Thompson et al., VCH, Weinhein, 2004.

$$V = F.T.[I'(\Theta)] = F.T.[A(\Theta)I(\Theta)] \tag{1.50}$$

In Fig. 33 it is shown that the resolution of an interferometer depends on the component of the distance between the two antennae in a direction perpendicular to the incoming radiation, the so called *baseline*. In interferometry we usually refer to *projected baselines*, measured as usual in wavelengths, *in the plane perpendicular to a reference direction*, that is the telescope pointing center (see Fig. 35). Baselines in this plane are specified by coordinates (u,v) (***uv-plane***) , where u is towards the East and v towards the North. The corresponding coordinates in the sky are directional cosines (x,y) relative to the u,v axes respectively.

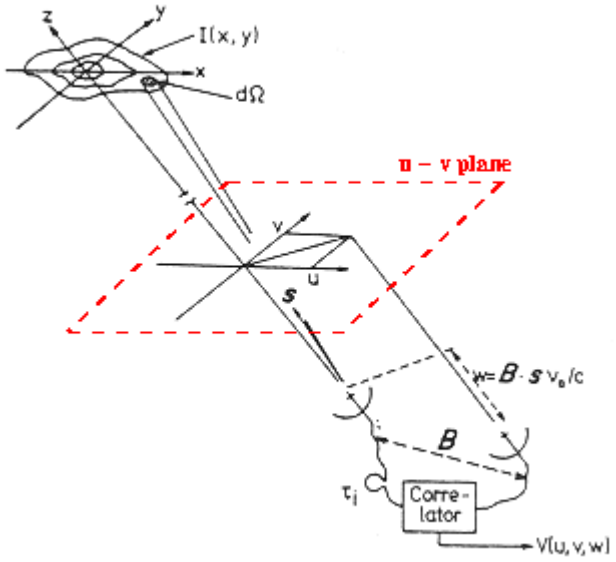


Figure 35: uv-plane and coordinates

Using this notation, we can write Eq. (1.50) as:

$$V(u,v) = \iint_{-\infty}^{+\infty} A(x,y)I(x,y)\,e^{-2\pi i(ux+vy)}\,dxdy \tag{1.51}$$

$$I'(x,y)=A(x,y)I(x,y)=\iint_{-\infty}^{+\infty} V(u,v)\,e^{2\pi i(ux+vy)}\,dudv \qquad (1.52)$$

However *the above equations are true only for the case of continuous sampling of the uv-plane such that* V *is measured for* ***all*** *values of* (u,v) . We know that the field radiation pattern related to the interference coming from two antennae is characterized by a single spatial frequency (Eq. (1.21)). Therefore, we can write that the visibility measured from each pair of antennae corresponds to one Fourier component of the modified sky $I'(x,y)$. Which Fourier component is measured by a pair of antennae is determined by their projected baseline. As it stands out clearly in an intuitive way and as we will detail a bit in the following, in order to get good images of astronomical sources we need to measure V for as many (u,v) pairs as possible (i.e. we need a good sampling of the *uv*-plane). Anyway, since there are always finite spacings possible between the antennae of an array, the *uv*-plane is sampled at discreet (u,v) points. We can thus define a s*ampling function*:

$S(u,v)=1$ at (*u,v*) points where visibilities are measured

$S(u,v)=0$ elsewhere

The sampling function is irregular and limited, and *the pattern of all measured (u,v) points is usually referred as the uv-coverage*. Due to this, Eq. (1.50) has to be re-written as:

$$\boldsymbol{V\times S=F.T.[I'*A_{dirty}]=F.T.[I_{dirty}]} \qquad (1.53)$$

where $\boldsymbol{I_{dirty}}$ is the ***dirty map*** and $\boldsymbol{A_{dirty}}$ is the ***dirty beam****, i.e.* is the point spread function of the whole interferometer. Based on the properties of F.T.s and on Eq. (1.50) we derive that:

$$S=F.T.(A_{dirty}) \qquad (1.54)$$

that is, *the sampling function is the F.T. of the dirty beam*. All what we have seen up to now is summarized in Fig. 36:

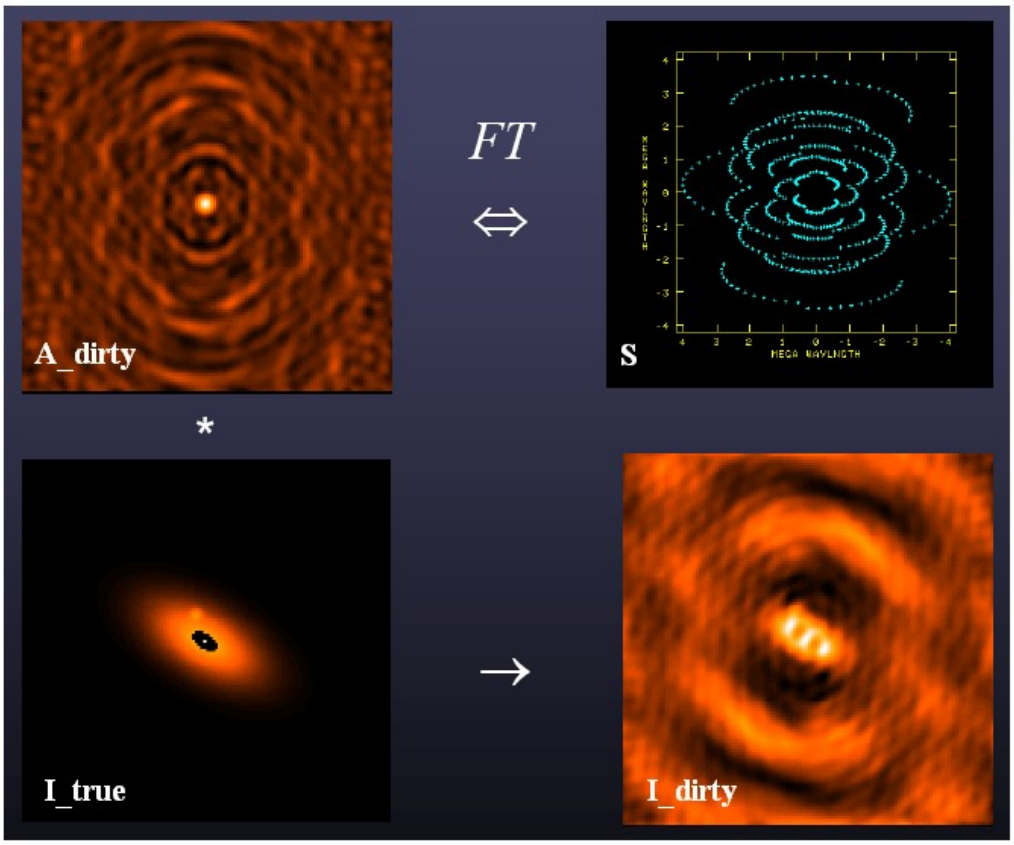


Figure 36: The dirty image (Eq. 1.53)

The shape of the dirty beam is a function of the *uv*-coverage which in turns is a function of the location of the antennae. The dirty beam for a fully covered *uv*-plane (that is not feasible at all, as already said) would be a *sinc* function (as in the case of the full aperture diffraction pattern). The width of the main lobe of this function is proportional to λ / u_{max}, where u_{max} is the maximum available baseline. For a real *uv*-coverage however, *S* is not at all flat till u_{max} and has "holes" in between representing un-sampled (*u,v*) points. The effect of the missing data is to increase the side lobes and make the dirty beam noisy, but in a determinate manner (see Figs. 38, 39 and 40).

Typically, a good enough coverage of the *uv*-plane ensures that an elliptical Gaussian can be fitted to the main lobe of the dirty beam (see Fig. 40) and is used as the resolution element of the telescope. The fitted Gaussian is referred to as the *synthesized beam*. As we will see very soon, we have to get rid as much as possible of the dirty beam. The closest to a Gaussian is the dirty beam, the easier if this task. It is thus clear from all what we said that ***we need to cover the uv-plane as well as possible in our observations***, i.e. ***we need to have many different antenna spacings.***

The use of a series of baselines, or the simultaneous use of many interferometer baselines of an array of telescopes, is called ***aperture synthesis***. The first method to have many different baselines is to connect arrays of several (N) radio telescopes, connected pairwise to give a collection of $N(N-1)/2$ baselines and thus visibilities V_{ij} (***aperture synthesis array***). If the number of antennae is sufficiently large, or if the source is sufficiently simple, a brief observation time may already provide a usable map (in terms of the resulting dirty beam). This is known as *snapshot* mode. However the number of antennae in an interferometer is severely limited by practical reasons, the first of them being the cost of the instrument. For increasing the number of baselines in radio observations we can therefore exploit the Earth rotation, which, for every single pair of antennae, provides a continuous arc of baselines. Actually, as the Earth rotates, the source sees different baselines lengths in the *uv*-plane (Fig. 37). This gives us the possibility to measure different Fourier components without moving antennae, but just increasing the observation time, and it is called ***Earth-rotation synthesis*** or ***super-synthesis***.

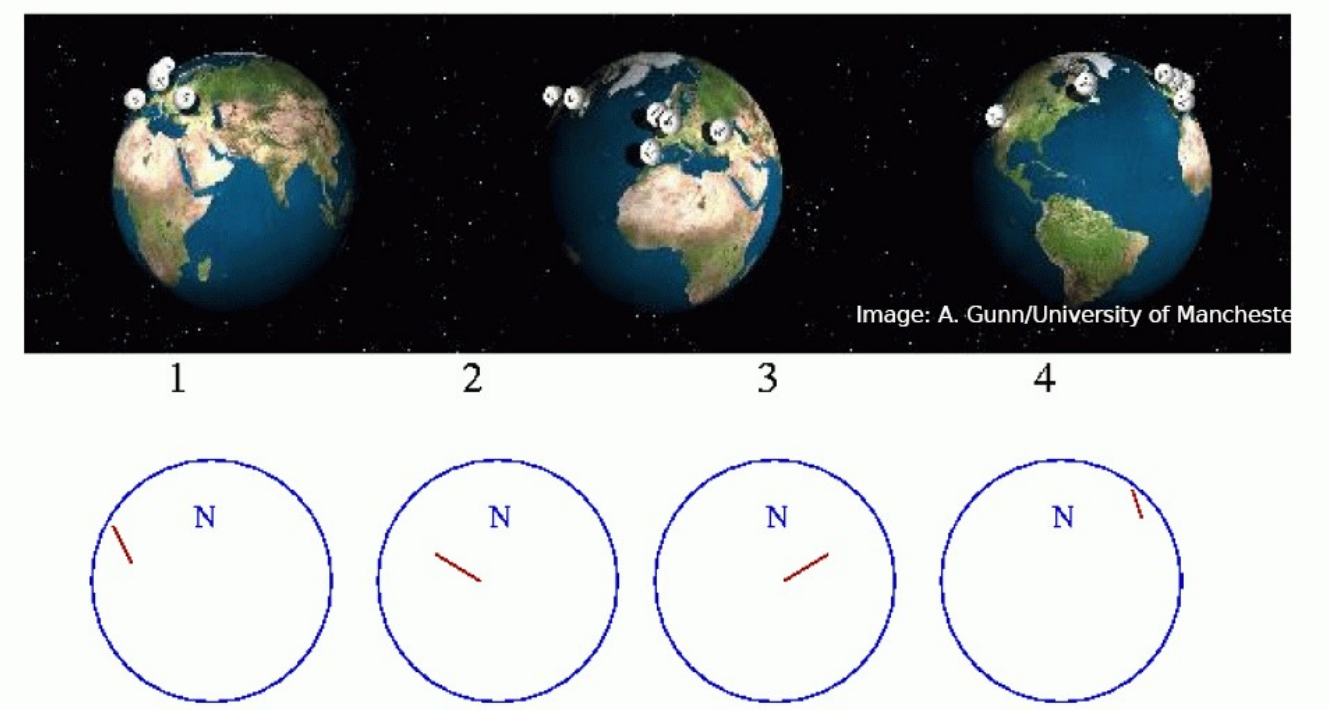


Figure 37: The track in the uv-plane traced out by a baseline due to the Earth's rotation

The evolution of the dirty beam obtained by firstly increasing the number of antennae, and secondly using super-synthesis is shown in Figs. 38, 39 and 40.

The dirty map is a convolution of the true brightness distribution and the dirty beam, and it is almost never a satisfactory final product since the side lobes of the dirty beam (due, as already said several times, to the missing spacings in the *uv*-domain) will contaminate the entire map at levels higher than the thermal noise (see for instance Fig. 41). As we will see in the next section, w*e have therefore to try to remove the effect of the dirty beam from the map before using it for astrophysical studies*.

Before concluding, a short summary of the basic lexicon in aperture synthesis:

- ***Baseline:*** line segment between two antennae (normally measured in a direction perpendicular to the telescope pointing direction)
- ***Configuration:*** layout of the antennae
- ***Beam:*** instrument diffraction pattern
- ***Primary beam:*** beam of the single antenna (single dish beam)
- ***Field of view of the interferometer:*** primary beam size
- ***Synthesized beam:*** beam of the interferometers
- ***Image resolution of the interferometer:*** synthesized beam size

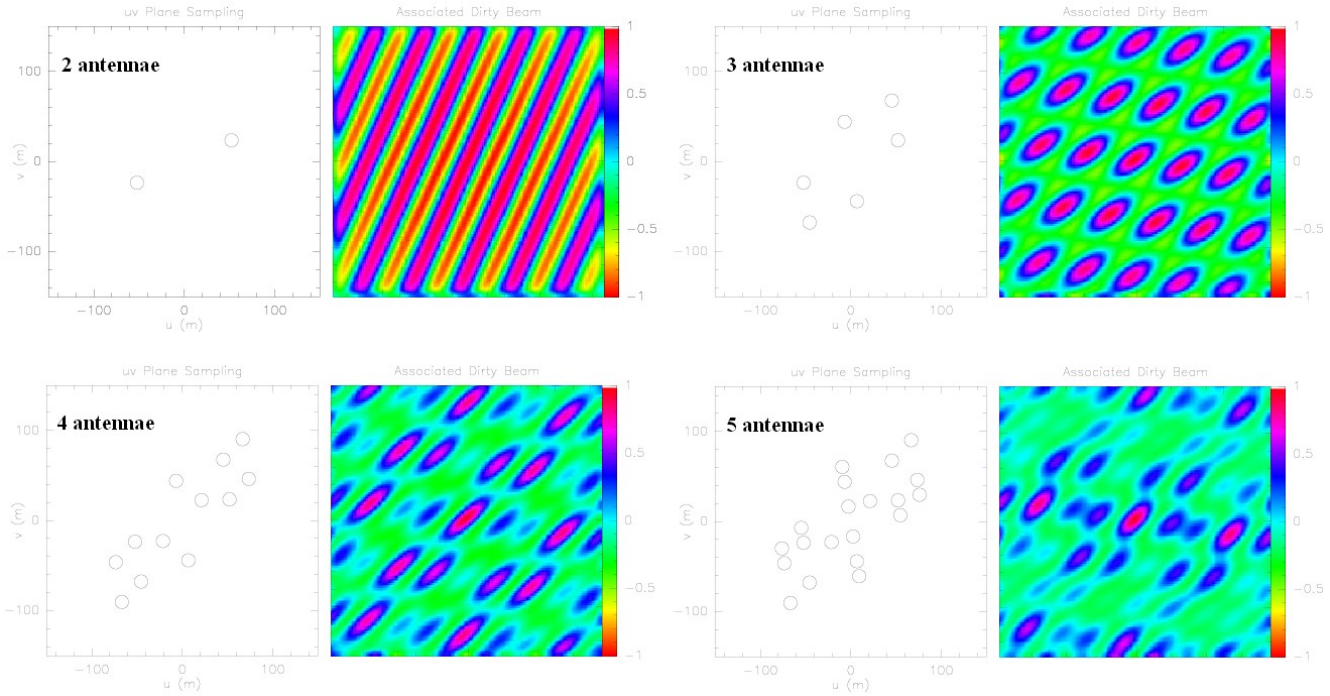


Figure 38: Dirty beam of interferometers with different numbers of antennae

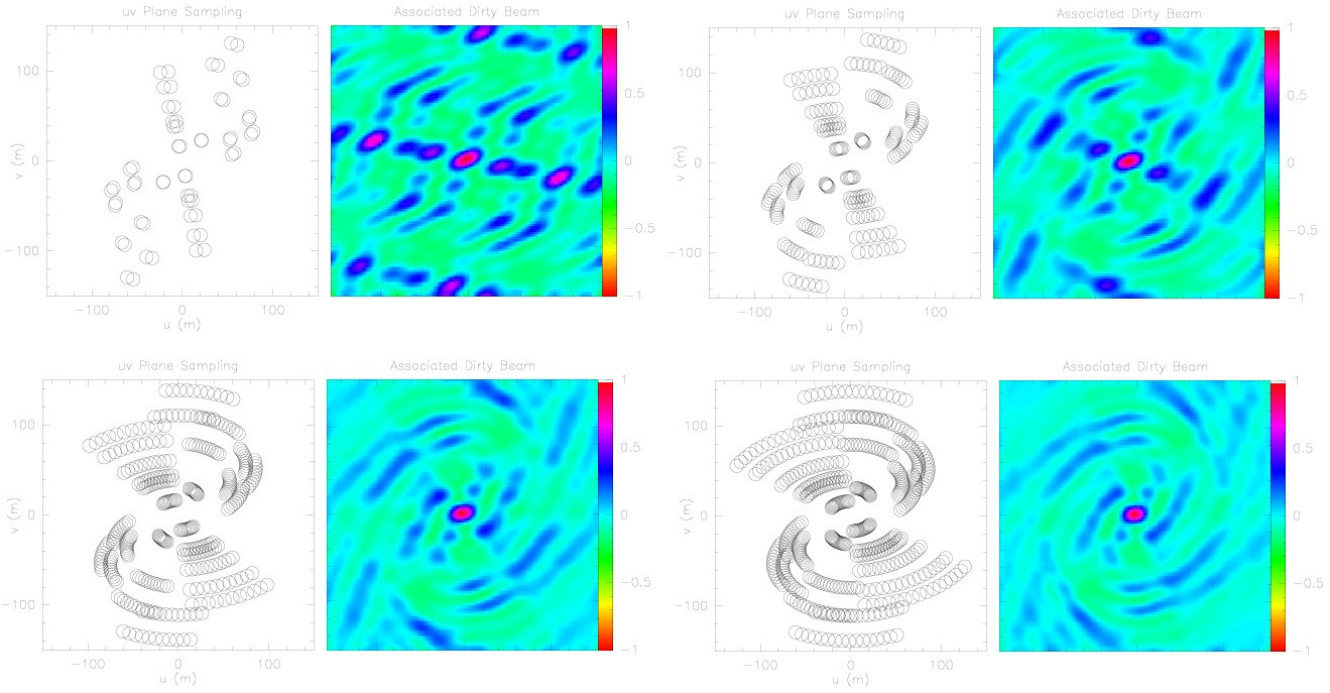


Figure 39: Dirty beam of an interferometer made up by N antennae for increasing observation times (from left to right and from top to bottom)

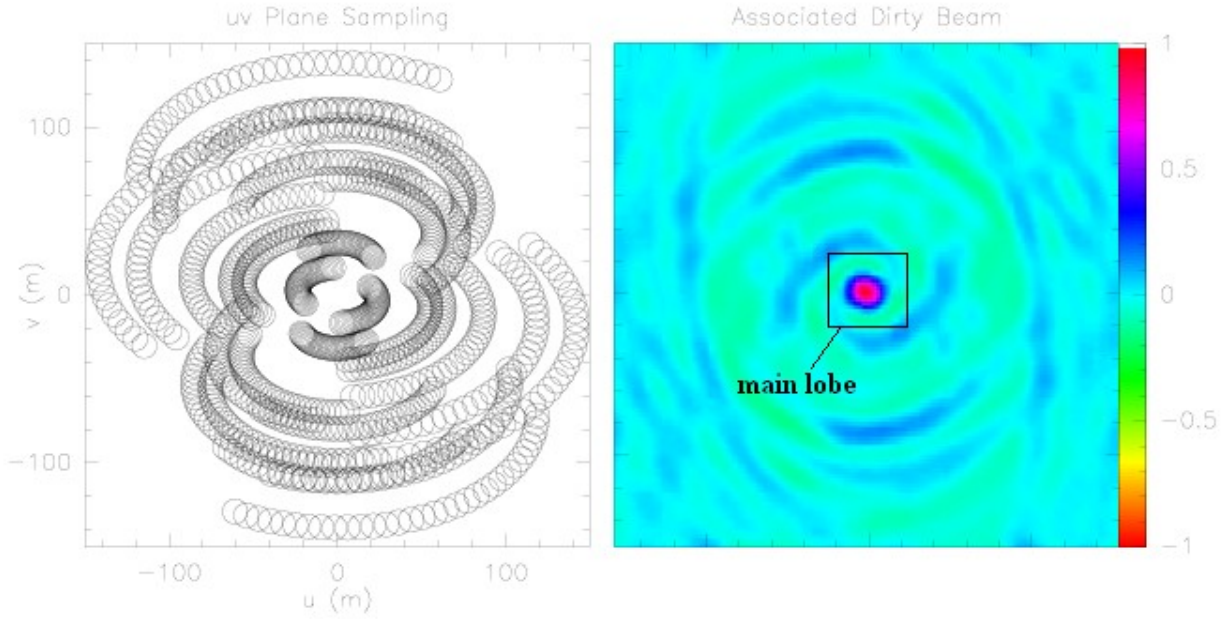


Figure 40: Dirty beam of an interferometer made up by N antennae and for a long observation time. The main lobe of the dirty beam can be fitted with an elliptical Gaussian

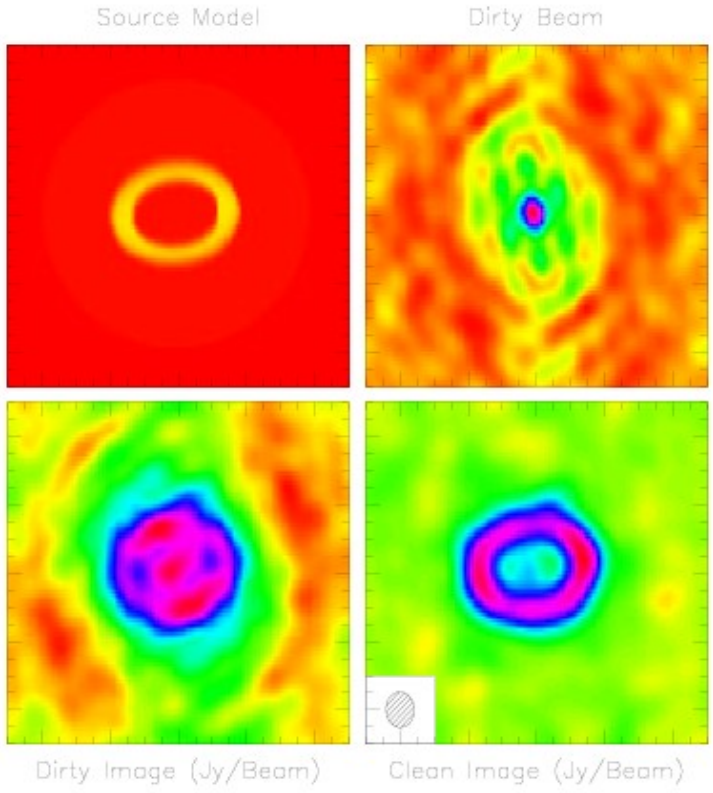


Figure 41: That's why we need deconvolution!!!

1.6.1 Imaging & Deconvolution

We have found (Eq. (1.53)) that:

$$V \times S = F.T.[I' \star A_{dirty}] = F.T.[I_{dirty}]$$

Based on the previous equation, once we have our observed visibilities we need to follow the steps given in Fig. 42 in order to get an image ready to be used for scientific analyses:

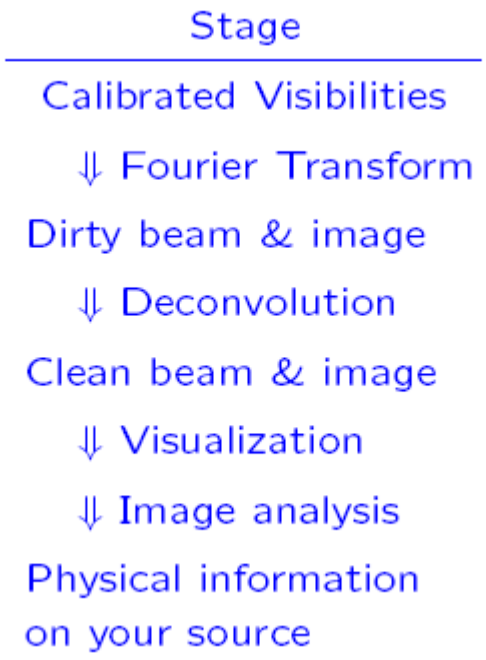


Figure 42: From observed visibilities to images ready for the scientific analysis

Again, we cannot enter in the details of the whole procedure, and I will try to give you just some basic ideas about making images from interferometric data. In particular, we will not have the time to see in details the very important first step concerning *visibility calibration*. Very shortly, we can say that we need to calibrate visibilities since, in reality, the output of our instrument is different from the astronomical visibility for a variety of reason, to do with both instrumental effects as well as propagation effects in the Earth's atmosphere and ionosphere. These effects can introduce phase delays into the incoming radiation on the different antennae. We can thus have a loss of coherence due to

instrumental and atmospheric factors, which implies that we do not measure the true visibility of the source. The measured visibility V_m is approximately given by the product of the true visibility V_t and a factor, called system visibility V_s, which represents the loss of coherence due to instrumental and atmospheric factors. We can derive V_s and hence V_t by observing calibration sources (*phase calibrators*) for which V_t is known. In order to be able to determine the absolute source flux density we also need to observe a calibrator of known flux (*amplitude calibrator*). While it is sufficient to do amplitude calibration only once during an observing run, phase calibrators must be re-observed several times during the night. The main requirement for selecting the best phase calibrator (among the list of possible sources available in specific tables) is that it has to be as close as possible to the target source, in order to have very similar wave distortions. The calibrator has also to be a bright source in order to get good S/N with reasonably short integration times.

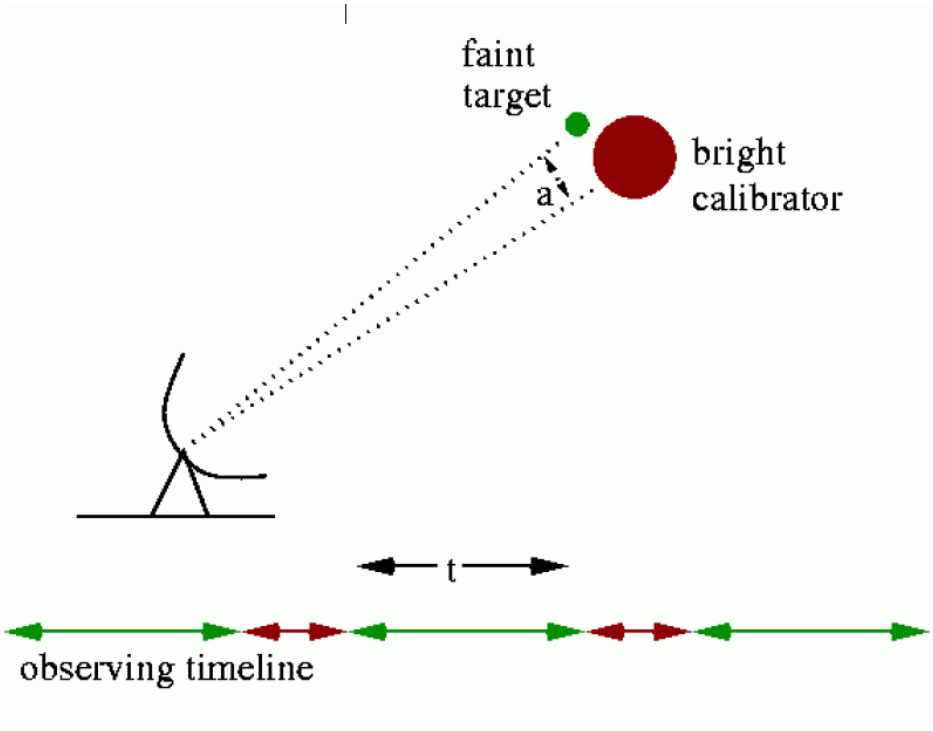


Figure 43: Sketch of observations for phase calibration

For what concerns the first step of the procedure in Fig. 42, i.e. the *Fourier transform* of the observed visibilities also called *imaging*, the simplest approach would be to directly compute *sin* and

cos functions in Eq. (1.53) for all combinations of visibilities and pixels in the image. This is straightforward, but slow. A typical data set from the Very Large Array (VLA), one of the best available radio telescopes, contains up to 10^5 visibilities per hour and usually require large images (1024×1024 pixels). The computation time can thus be prohibitive.

In practice, everybody uses the Fast Fourier Transform (FFT) because of its definite speed advantage. The drawback of the methods is the need to re-grid the visibilities (which are measured at arbitrary points in the (*u*,*v*) plane) on a regular grid to be able to perform a 2-D FFT. It has been shown that this gridding process introduce some distortion in the dirty image and dirty beams, which should be corrected afterwards. Moreover, since the gridded visibilities are sampled on a finite ensemble, an *aliasing* of the dirty image (and beam) in the map plane is introduced. This means that FFT introduces a folding of intensity outside the image size into the image, as shown schematically in Fig. 44.

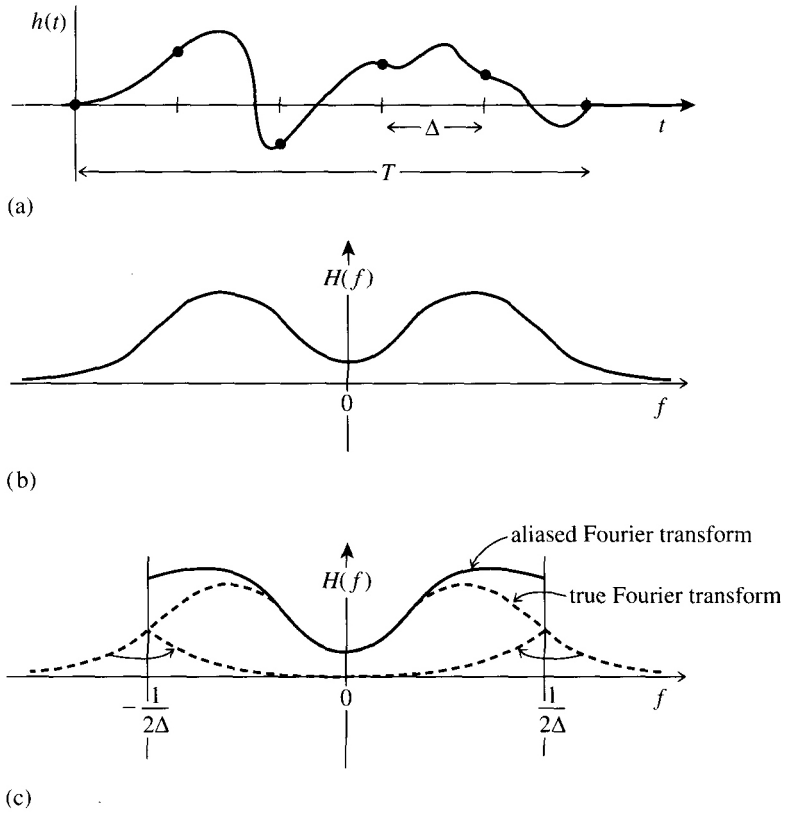


Figure 44: Aliasing introduced by the FFT of the observed visibilities

Deconvolution is also a very delicate stage, that has to remove as much as possible the noise due to

the dirty beam and introduced by the previous step (FFT). The closest to a Gaussian the dirty beam is (i.e. the better is the *uv*-coverage), the easier the deconvolution. The basic idea of deconvolution, proposed in 1974 by J. Högbom and subsequently developed and improved, is summarized in the following (text taken from the WEB page of the Giant Metrewave Radio Telescope - GMRT[11]) and schematically shown in Figs. 45, 46, 47 and 48:

" Consider a sky containing only isolated point sources. In the dirty map, each appears as a copy of the dirty beam, centered on the source position and scaled by its strength. However, the maxima in the map do not strictly correspond to the source positions, because each maximum is corrupted by the side lobes of the others, which could shift it and alter its strength. The least corrupted, and most corrupting, source is the strongest. Why not take the largest local maximum of the dirty map as a good indicator of its location and strength? And why not subtract a dirty beam of the appropriate strength to remove to a great extent the bad effects of this strongest source on the others? The new maximum after the subtraction now has a similar role. At every stage, one writes down the co-ordinates and strengths of the point sources one is postulating to explain the dirty map. If all goes well, then at some stage nothing (or rather just the inevitable instrumental noise) would be left behind. *We would have a collection of point sources, the so called CLEAN components, which when convolved with the dirty beam give the dirty map*. One could exhibit this collection of point sources as the solution to the deconvolution problem, but this would be arrogant, since one has only finite resolution. As a final gesture of modesty, *one replaces each point source by (say) a Gaussian, a so called "CLEAN" beam, and asserts that the sky brightness, convolved with this beam, has been found.* "

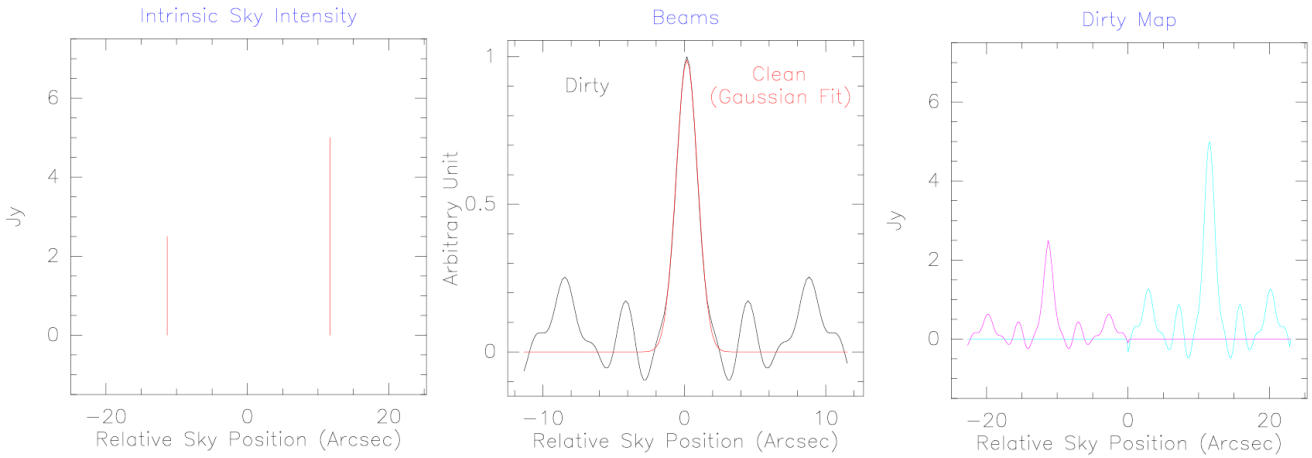


Figure 45: Simple illustration of the basic clean algorithm: part I

11 http://www.gmrt.ncra.tifr.res.in/

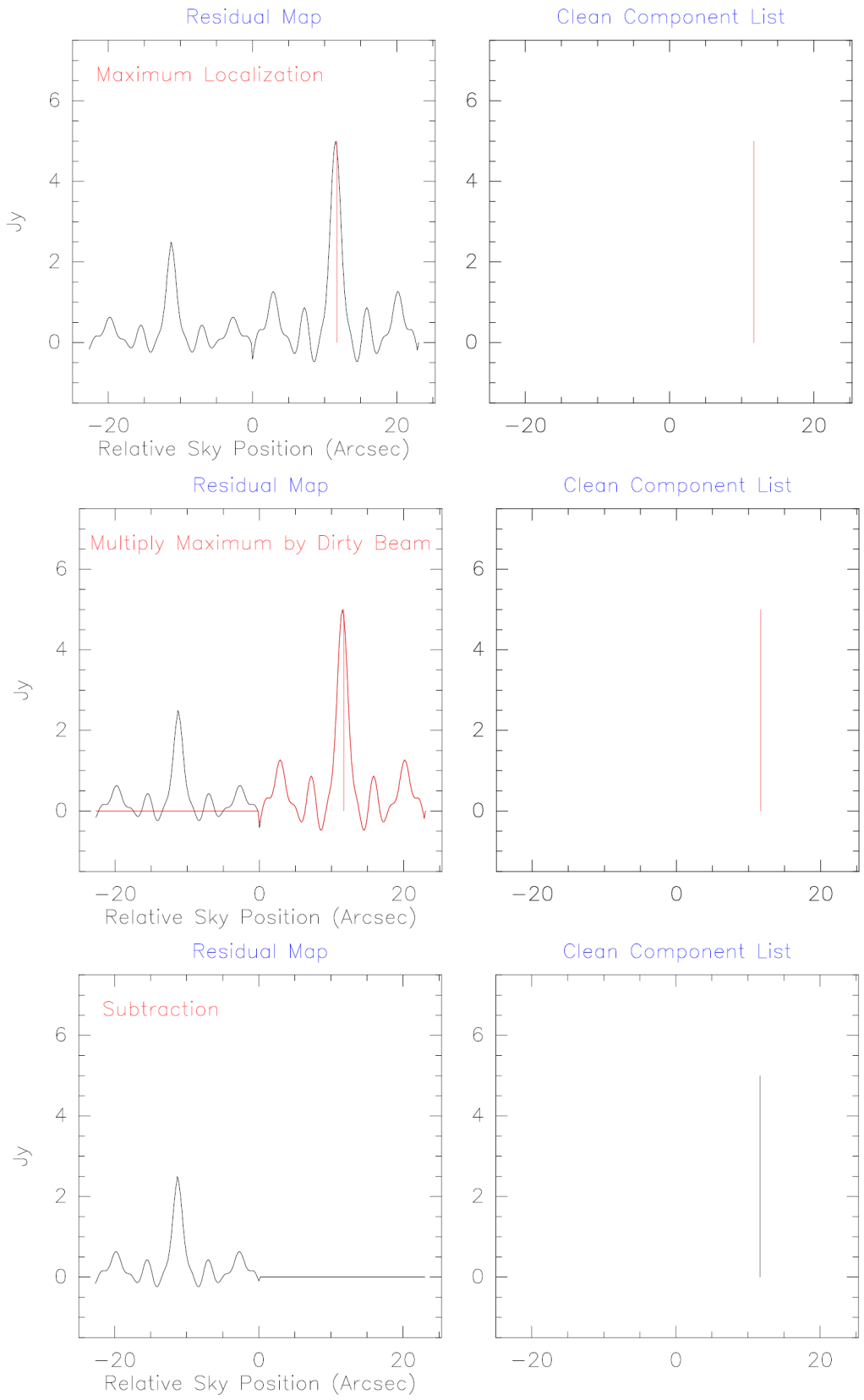


Figure 46: Simple illustration of the basic clean algorithm: part II

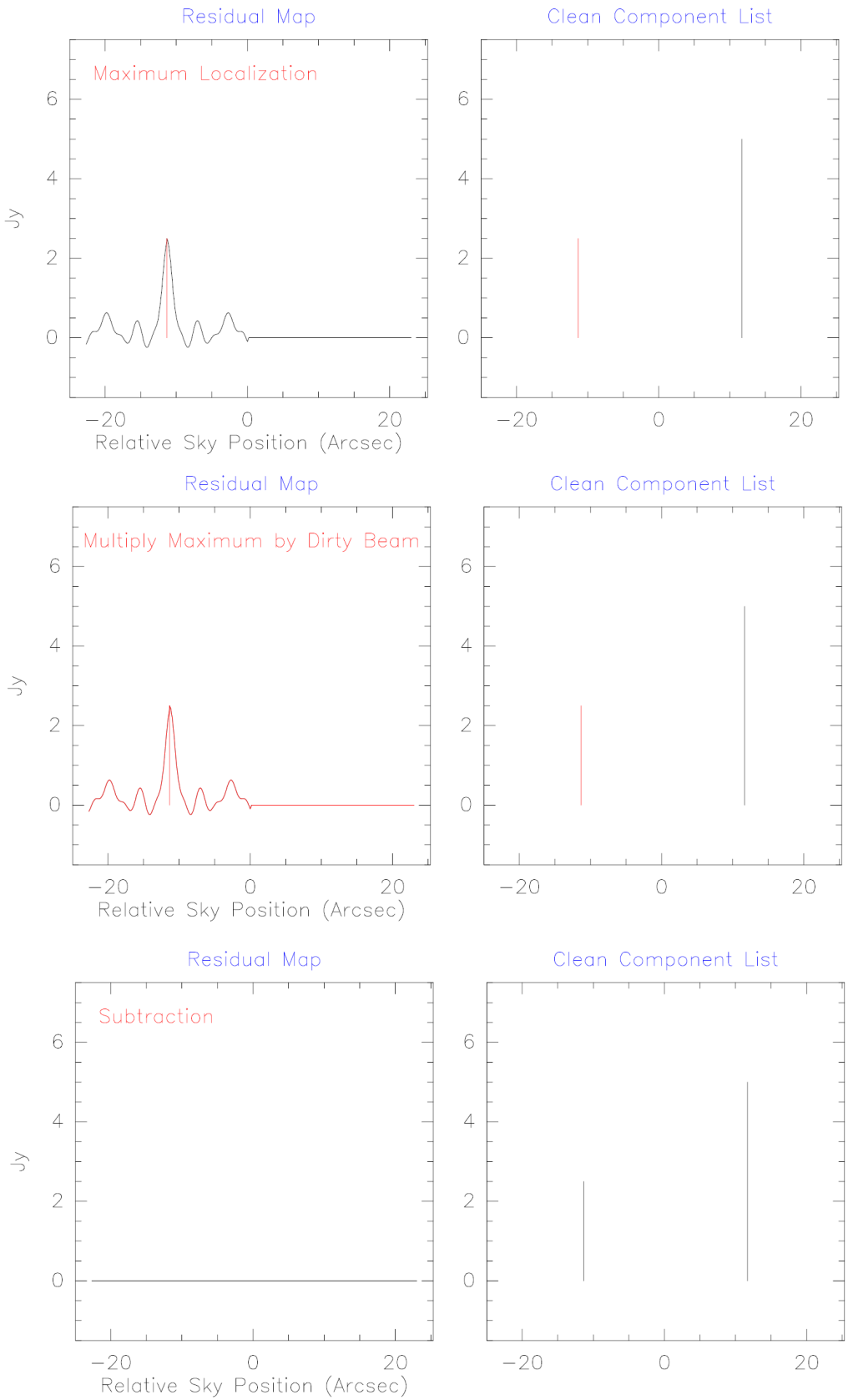


Figure 47: Simple illustration of the basic clean algorithm: part III

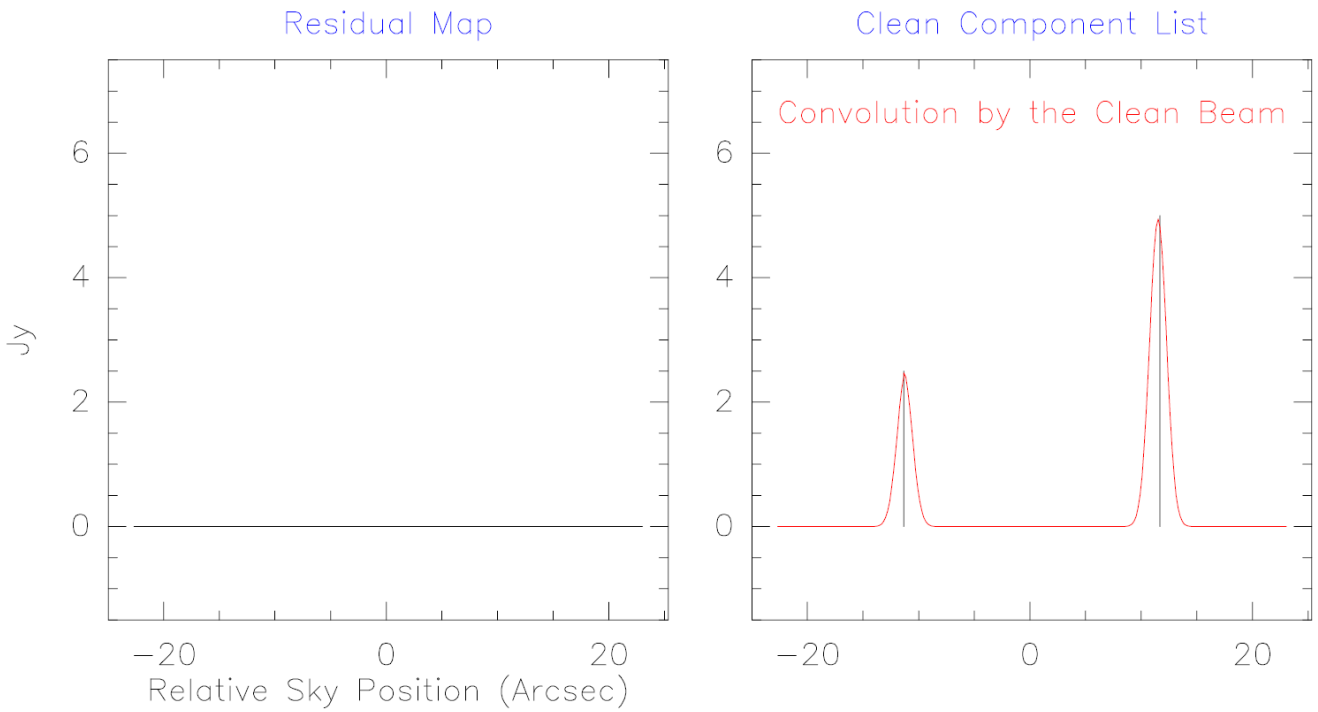


Figure 48: Simple illustration of the basic clean algorith: part IV

The imaging and deconvolution procedures, bringing from the observed visibilities to the final image on which we can work, are very well summarized in Figs. 49 and 50 respectively:

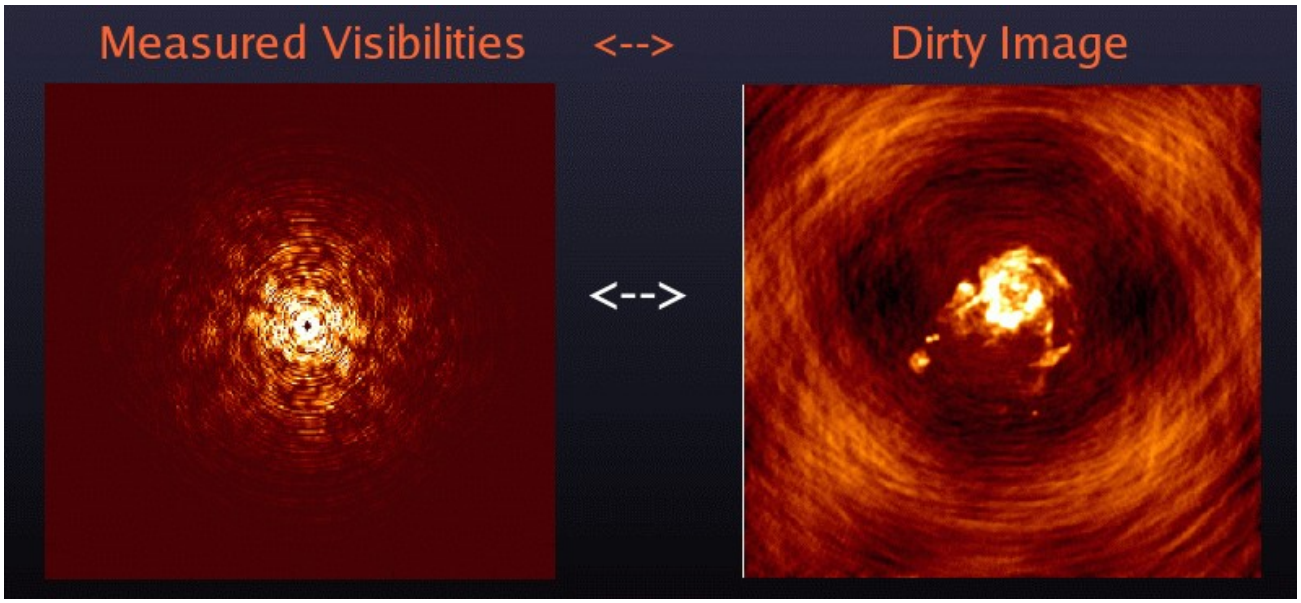


Figure 49: Imaging

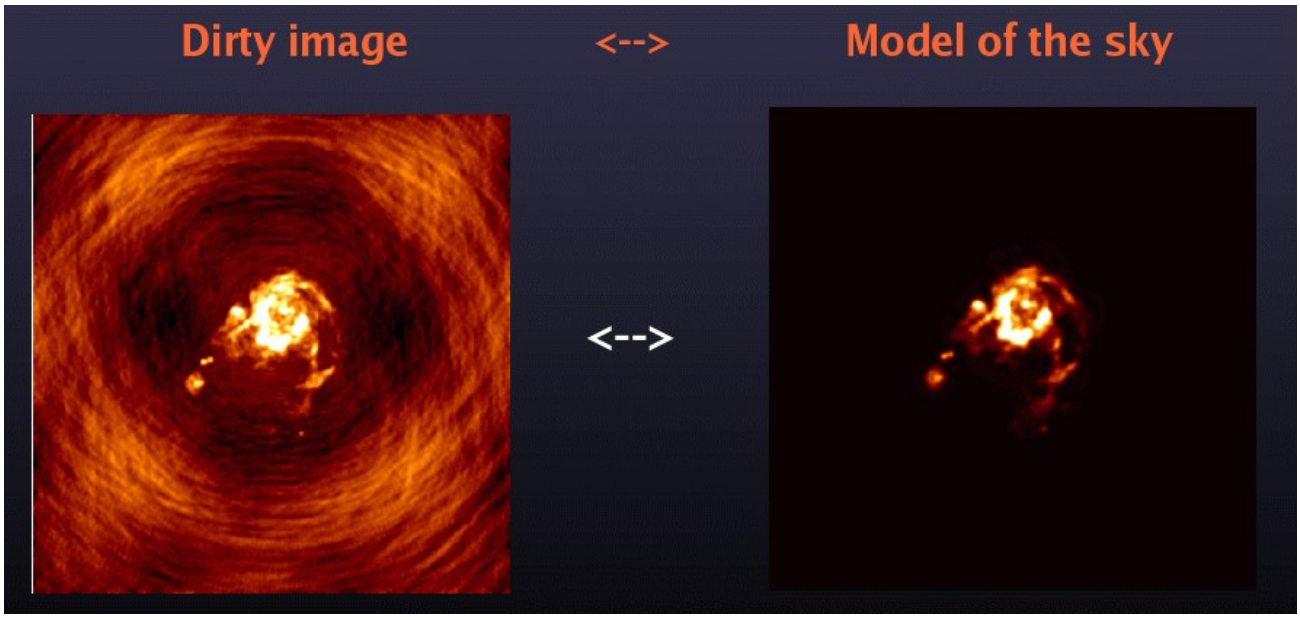


Figure 50: Deconvolution

We conclude with some pictures of some of the most important radio telescopes available at present, both single dishes and interferometers.



Figure 51: The 76 m Lovell radio telescope at Jodrell Bank Observatory



Figure 52: The largest radio telescope in Europe: the 100 m diamtere antenna in Effelsberg



Figure 53: The world's largest (~90 m) fully steerable radio telescope: Green Benk (USA)



Figure 54: The 305 m Arecibo radio telescope



Figure 55: The Very Large Array (VLA): 27 antennae with a diamter of 25 m, arrayed along three arms of a Y-shape, each of which measures 21 km. The maximum baseline is 36 km (Socorro, USA)

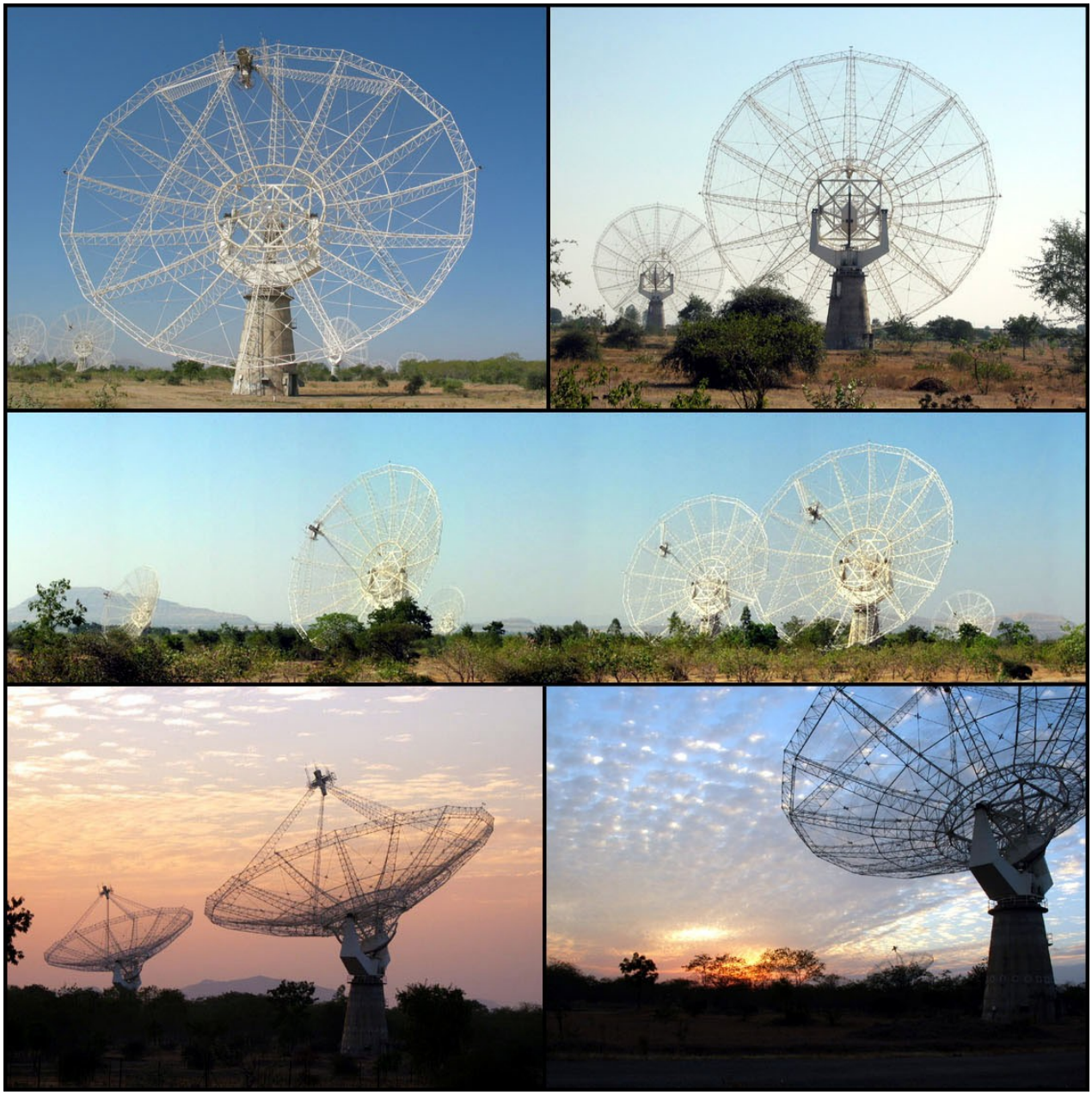


Figure 56: The world's largest radio telescope at meter wavelengths: the GMRT (Pune, India). There are fourteen telescopes randomly arranged in the central square, with a further sixteen arranged in three arms of a "Y"-shaped array (similar to the VLA) giving an interferometric baseline of about 25 km.



Figure 57: The Australia Telescope Compact Array – ATCA (Narrabri, Australia). The telescope is an array of six identical 22 meter diameter dishes. Five of the dishes can be moved along a three kilometer railway track. The sixth antenna is situated three kilometers west of the end of the main track.

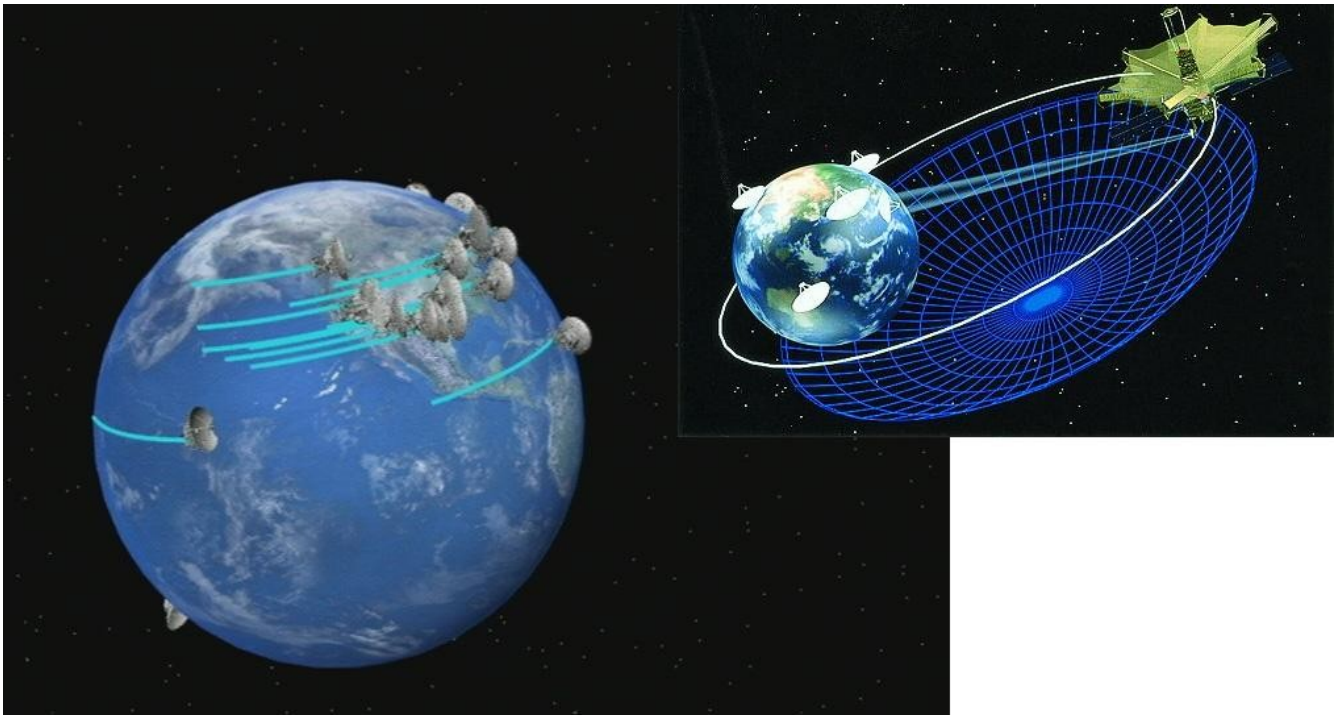


Figure 58: Very Long Baseline Interferometry (VLBI) is a type of astronomical interferometry used in radio astronomy, in which the data received at each antenna in the array are paired with timing information, usually from a local atomic clock, and then stored for later analysis on magnetic tape or hard disk. At that later time, the data are correlated with data from other antennas similarly recorded, to produce the resulting image. The resolution achievable using interferometry is proportional to the observing frequency and the distance between the antennas furthest apart in the array. The VLBI technique enables this distance to be much greater than that possible with conventional interferometry, which requires antennas to be physically connected by coaxial cable, wave guide, or other type of transmission lines. The latest development in radio astronomy observations is the Space Very Long Baseline Interferometry (SVLBI) program. This is used to perform radio astronomy with an extended baseline VLBI, of which one element is a space-based antenna (extracted from Wikipedia).